Master Thesis in Geographical Information Science nr 203

Detecting Structurally Old Scots Pine

A Crown-Metric Approach Using National ALS and LIFT Enrichment

Simon Westman

2026
Department of
Physical Geography and Ecosystem Science
Centre for Geographical Information Systems
Lund University
Sölvegatan 12
S-223 62 Lund
Sweden

Simon Westman (2026). Detecting Structurally Old Scots Pine: A Crown-Metric Approach Using National ALS and LIFT Enrichment.
Master degree thesis, 30 credits in Geographical Information Systems (GIS)
Department of Physical Geography and Ecosystem Science, Lund University

Detecting Structurally Old Scots Pine: A Crown-Metric Approach Using National ALS and LIFT Enrichment

---

Simon Westman

Master thesis, 30 credits, in Geographical Information Sciences
Lund University

Supervisor

Jonas Ardö
Department of Physical Geography and Ecosystem Science
Lund University

Abstract

Old Scots pine trees provide important habitat structures in forest ecosystems, but intensive forest management in Sweden has made them increasingly rare and difficult to locate across large areas. Field inventories are reliable but costly and limited in extent, creating a need for scalable methods to support retention forestry. This thesis develops and evaluates a method for identifying Scots pine trees with old-like structural characteristics using nationally available airborne laser scanning (ALS) data. Individual tree crowns were segmented, and tree height, crown diameter, crown flatness and height growth were derived from multi-temporal ALS data. To account for site-related differences, trees were compared within environmentally similar strata based on elevation, soil moisture and peat depth. An enrichment-based threshold analysis using the LIFT ratio was then applied to identify old-like structural patterns. The method was developed in the Idre–Särna area and tested in the Lunsen–Kungshamn–Morga landscape outside Uppsala. The results show that clear enrichment patterns were detected in a limited number of strata, mainly on dry-fresh mineral soils. Predicted old-like trees represented well below 1% of crowns and a small field validation showed high precision but moderate recall (0.37). Overall, the method functions as a reliable prioritization tool for helping field surveys toward structurally mature Scots pine using national ALS data.

Keywords: Geography, Geographical Information Systems, GIS, Airborne Laser Scanning (ALS), Scots pine, Structural ageing, Crown segmentation, LIFT analysis

Acknowledgements

I would like to express my sincere gratitude to Skogforsk (the Forestry Research Institute of Sweden) for their collaboration and support throughout this thesis. They provided the canopy height models, guidance on relevant data, continuous support through meetings and emails, and practical help during the field validation.

I would like to especially thank Maria Nordström, Per Westerfelt and Linn Gäfvert at Skogforsk. They welcomed me into the organization, were always responsive and open to discussion, and taught me the importance of having multiple tablets during cold field days.

All three contributed generously with their time, ideas and practical support, and played an important role in enabling this thesis.

Table of Contents

List of Figures

List of Tables

List of Abbreviations and Translations

Abbreviation	**Definition**
ALS	Airborne Laser Scanning
DEM	Digital Elevation Model
CHM	Canopy Height Model
P95	95th percentile
SLU	Swedish University of Agricultural Sciences
Lantmäteriet	The Swedish Mapping, Cadastral and Land Registration Authority
Naturvårdsverket	The Swedish Environmental Protection Agency
Skogsstyrelsen	The Swedish Forest Agency

1. Introduction

Structurally old trees play an important role in boreal forest ecosystems. Their large crowns, rough bark and broken branches create habitats that many species depend on, and these features take a very long time to develop (Siitonen, 2001). In Sweden, long-term intensive forest management has greatly reduced the number of structurally old trees, leading to forests that are younger and more uniform than they once were (Linder, 1998; Skogsstyrelsen, 2020). Because old trees are now rarer, being able to find and retain them is important for conservation-focused forestry. However, traditional field inventories are time-consuming, expensive and limited to small areas. This makes it difficult to identify old trees across large forest landscapes (Fridman et al., 2014).

Airborne Laser Scanning (ALS) offers a practical alternative. National ALS data are available across most of Sweden and are widely used in forestry planning and mapping (Nilsson et al., 2016; Skogsstyrelsen, 2020). ALS captures the three-dimensional structure of the forest canopy, which makes it possible to measure tree height, crown size and crown shape. These features are known to change as Scots pine (*Pinus sylvestris* L.) ages, leading to slower height growth, wider and flatter crowns, and more irregular structures (Holmgren & Persson, 2003; Saarinen et al., 2022; Huo et al., 2023). When ALS data are available for more than one point in time, changes in tree height can also be used to estimate growth, which is another indicator of structural ageing.

Despite this potential, existing methods depend on high-density LiDAR data, multispectral sensors or local calibration, limiting their usefulness for national ALS datasets (Bonnet et al., 2015; Hirschmugl et al., 2023). Most operational approaches also focus on stand-level properties instead of individual trees, meaning that single old trees within managed stands are often overlooked (Breidenbach & Astrup, 2014; Schumacher et al., 2020). In addition, national ALS data have relatively low point density, which makes it difficult to capture fine crown details (Nilsson et al., 2016).

These limitations highlights the need for a method that makes better use of existing national ALS data to identify structurally old trees at individual tree level. This thesis addresses that need by developing and evaluating a method based on crown-level metrics derived from multi-temporal national ALS data. By combining site-based stratification with a statistical enrichment approach (LIFT), the goal is not to map all old trees, but to reliably identify a limited set of trees with strong old-like structural features (Han et al., 2012). In practice, this provides a scalable tool that can help guide field surveys and support retention forestry by indicating where structurally mature Scots pine are most likely to occur.

1.1 Problem Statement

Retention forestry requires reliable identification of structurally mature trees, but current inventories are largely based on field surveys that are expensive, time-consuming, and difficult to apply consistently across large forest holdings (Fridman et al., 2014). As a result, old and ecologically valuable Scots pine individuals risk being overlooked during operational planning.

Although national ALS data provide wall-to-wall information on forest structure, existing approaches are either developed for local calibration, require high-density data or operate at the stand level rather than individual trees (Bonnet et al., 2015; Hirschmugl et al., 2023). This limits their usefulness for detecting individual old trees using national datasets. There is therefore a need for a reproducible and efficient method that uses available national ALS data to identify Scots pine individuals with old-like structural traits.

1.2 Research Aim and Questions

The aim of this thesis is to develop and test a method for identifying Scots pine crowns with structural features that are typical of old trees, using multi-temporal ALS data. The goal is to support forestry and conservation planning by helping to identify areas where old trees are more likely to occur.

Q1: How effectively can ALS-derived canopy metrics be used to detect old-like structural traits in Scots pine across heterogeneous forest landscapes?

Q2: How do selected canopy-metric thresholds differ among site-based groups?

Q3: How accurately does the canopy-based thresholds identify old Scots pine individuals when assessed through field validation?

1.3 Thesis Contribution

This thesis makes both methodological and practical contributions to the identification of old-like Scots pine using national ALS data.

From a methodological perspective, the thesis presents a transparent and reproducible workflow for extracting crown-level structural metrics from multi-temporal ALS data. A key contribution is the combination of crown metrics with site-based stratification and a simple statistical enrichment measure (LIFT). LIFT is used to identify combinations of canopy features that occur more often than expected by chance. This makes it possible to detect old-like tree structures while accounting for local variation. Together, this allows old-like crowns to be identified relative to their local environment, rather than using fixed thresholds across the whole landscape. The thesis also evaluates the strengths and limitations of using national ALS data for tree-level ageing.

From a practical perspective, the thesis provides a decision-support approach that can help forest owners and planners prioritize field surveys and identify trees that bear the strongest signal of structurally old Scots pine. Because the method only relies on existing national data, it can be applied without additional data collection and integrated into current forestry workflows. This shows how routinely collected remote sensing data can be used to support retention forestry and conservation planning while reducing the need for extensive field inventories.

2. Background

The background provides the ecological and scientific context for the thesis. It describes why old trees are important for forest ecosystems, how ageing is expressed in Scots pine, how ALS has been used to study forest structure, and the statistical core of the method. Together, this background explains why the method in this thesis is relevant and needed.

2.1 Old Trees and Structural Ageing in Scots Pine

Although old trees are ecologically important, defining what an "old" tree is not straightforward. Tree age is difficult to measure accurately in practice. Increment cores (thin wood sample taken from the stem to study a tree's age) may miss the pith of the tree, contain false rings or be impossible to collect in protected or sensitive areas (Helms, 2004). In addition, tree size is not a reliable indicator of age. Some trees grow large quite fast under good conditions, while very old trees may remain small on poor or dry sites (Helms, 2004). Because of these limitations, many studies focus on structural characteristics rather than chronological age when identifying old trees. These structural characteristics consist of crown shape, bark texture, dead branches and irregular growth patterns (Huo et al., 2023). In Scots pine, ageing is commonly expressed through reduced height growth, lateral crown expansion and increasingly flattened or irregular crowns (Saarinen et al., 2022; Huo et al., 2023).

In Sweden, centuries of forest management have greatly reduced the number of old trees. Clearcutting, thinning and even-aged forestry have created forests that are younger and structurally more uniform than historical conditions (Linder, 1998; Skogsstyrelsen, 2020). Today, old trees are scarce and often found only in protected areas, low-productive sites or remnant patches (Skogsstyrelsen, 2020). This makes them important for biodiversity conservation, but also difficult to locate across large, forested landscapes.

Field inventories can identify old trees accurately, but they are expensive and cover limited areas. At the same time, most operational forest data in Sweden are designed for stand-level assessments rather than individual trees (Nilsson et al., 2016). This gap highlight the need for methods that can identify structurally old trees using operational data (Hirschmugl et al., 2023).

2.2 Age-Related Structural Traits of Scots Pine

Scots pine (*Pinus sylvestris* L.) is one of the most widespread tree species in Sweden and can reach ages of several hundred years under natural conditions (Linder, 1998). As pine trees age, their growth pattern changes gradually. Height growth slows down, the main leader becomes less dominant, and growth increasingly occurs sideways through crown expansion (Saarinen et al., 2022). These changes reflect both biological ageing and long periods of canopy dominance. Over time, older pines often develop wider and flatter crowns, irregular shapes and reduced annual height growth (Huo et al., 2023). These traits are not tied to a specific age but is part of a long structural development progress.

Because these changes affect the three-dimensional structure of the canopy, they are potentially detectable using airborne laser scanning. ALS captures both vertical and horizontal aspects of

tree crowns, making Scots pine a suitable species for testing whether structural ageing can be identified using remote sensing data.

2.3 Airborne Laser Scanning for Structural Forest Assessment

ALS provides three-dimensional information about forest structure by measuring how laser pulses reflect off vegetation and the ground. From these measurements, canopy height models (CHMs) and many structural metrics can be derived (Vauhkonen et al., 2014). In Sweden, Lantmäteriet (the Swedish Mapping, Cadastral and Land Registration Authority) conducts repeated nationwide ALS campaigns that provide wall-to-wall coverage of the country. These datasets typically have point densities of 0.5–1.0 points per square meter and form the basis for several forest products (Nilsson et al., 2016). Although scans are not collected at fixed time intervals, repeated acquisitions make it possible to study changes in forest structure over time (Lantmäteriet, 2024a). Structural metrics such as tree height, and crown-related measures can all be derived from ALS-data and have widely been used to describe forest development and structural complexity (Holmgren & Persson, 2003; Næsset, 2002). When multi-temporal ALS data are available, changes in height can be used to estimate growth, which is useful for identifying trees with reduced growth rates associated with ageing (Kozniewski et al., 2022; Gavilan-Acuna et al., 2025).

At the same time, national ALS data has its limitations. Compared to research-grade LiDAR, point density is lower, and the resulting CHM models are therefore coarser. This makes it more difficult to capture fine-scale crown features (Nilsson et al., 2016). In dense or mixed stands, individual crowns can be hard to separate and small or suppressed trees may be poorly represented. These limitations make individual tree analyses challenging and reduce the direct transferability of methods developed using high-quality LiDAR data (Vauhkonen et al., 2014).

Despite these constraints, national ALS datasets are widely available and represent the baseline data used by forestry organizations and authorities. This makes it valuable to explore how much information about tree ageing can be extracted from these datasets, especially for usage across large areas where more detailed data are not available.

2.4 Limitations of Existing Approaches and Motivation for This Study

Remote sensing has improved forest monitoring, but identifying old trees is still difficult. Many advanced methods rely on high-resolution or multispectral LiDAR, which limits their applicability to small study areas and makes them unsuitable for use across larger areas (Bonnet et al., 2015; Hirschmugl et al., 2023). Many approaches also work at stand or plot level, where canopy metrics are averaged. As a result, single old trees within younger managed stands are often missed (Breidenbach & Astrup, 2014; Schumacher et al., 2020).

As stated previously, national ALS datasets have lower point density than research-grade LiDAR, but they represent the data that all forestry organizations have access to. These datasets are openly available, cover large areas and are already used in forest planning and inventory

work (Nilsson et al., 2016; Skogsstyrelsen, 2020). Because of this, national ALS data form a practical baseline for developing methods that can be applied without additional data collection.

Existing national products, such as SLU's age maps, estimate average stand age at pixel level. These products perform well in younger forests but tend to underestimate age in older stands, to the point where these maps cannot be used to identify older forests at landscape level (SLU, 2025). This limits their usefulness for detecting very old stands, which are often the most important for conservation work.

Together, these limitations point a clear need: a simple, transferable method that uses nationally available ALS data to identify trees with old-like structural characteristics at individual-tree level. Developing such a method would support retention forestry and improve the ability to locate ecologically valuable trees across large forest landscapes.

2.5 Enrichment-Based Thresholding (LIFT)

Detecting structurally old trees requires identifying combinations of structural traits that occur more frequently than expected by chance. To do this, the method uses the LIFT ratio, a measure of enrichment commonly applied in data mining (Han et al., 2012).

LIFT compares how often a certain combination of traits actually appears in the data (observed prevalence) with how often it would be expected to appear under a null model where the traits are assumed to be statistically independent (expected prevalence):

$$LIFT = \frac{Observed\ prevalence\ (O)}{Expected\ prevalence\ (E)} \qquad \text{Equation 1}$$

A LIFT value greater than 1 means that the trait combination occurs more often than random chance would suggest, indicating a meaningful structural pattern.

2.5.1 Expected Prevalence

Expected prevalence is calculated by multiplying the proportion of trees that meet each individual threshold, assuming the traits are independent. In this context, thresholds are defined to reflect structural characteristics associated with old-like Scots pine: relatively tall trees, wide crowns, low recent height growth and flat crown shapes.

For example, if:

- 40% of trees meet the height threshold
- 20% meet the crown diameter threshold
- 30% meet the growth threshold
- 10% meet the flatness threshold

The expected prevalence is:

$$E = 0.4\ x\ 0.2\ x\ 0.3\ x\ 0.1 = 0.0024\ or\ 0.24\% \qquad \text{Equation 2}$$

This means that, under the independence assumption, only 0.24% of trees would be expected to meet all four thresholds at the same time.

2.5.2 Observed Prevalence

Observed prevalence is the actual proportion of trees that meet all thresholds at the same time:

$$O = \frac{n_{selected}}{n_{total}} \quad \text{Equation 3}$$

Where:

- $n_{selected}$ is the number of crowns meeting all four criteria.
- n_{total} is the total number of crowns in the stratum.

Because canopy metrics are often related, like tall trees may also grow more slowly, the observed prevalence can be much higher than the expected value.

2.5.3 Interpretation

If the observed prevalence is higher than expected, LIFT becomes greater than 1. This indicates that the traits co-occur more often than random chance and that the combination represents a distinct structural pattern, consistent with old-like tree structures. A simple way to understand LIFT values is presented in Table 1:

Table 1: How to interpret LIFT values.

LIFT Value	Interpretation
< 1.0	Occurs less often than expected: filters need adjusting
= 1.0	Occurs as often as random: no distinct signal
> 1.0	Occurs more often than expected: positive enrichment
> 2.0	Strong enrichment: clear structural pattern indicating potential old tree

The independence assumption does not imply that canopy metrics are truly unrelated, but serves as a null model against which enriched trait combinations can be identified.

This enrichment-based approach offers two advantages over fixed thresholds:

1. It adapts to local site conditions by using percentile-based thresholds rather than global cut-offs.
2. It highlights structural niches rather than extreme values in a single variable. This is essential because ageing signals emerge through trait combinations rather than isolated metrics.

By applying LIFT within site-based strata, the method accounts for local variation and identifies structural patterns likely linked to ageing rather than site productivity. An example of how LIFT works is presented in appendix E.

2.6 Conceptual Framework

The idea behind this study is that structurally old Scots pine trees share certain crown characteristics that can be measured using ALS. To capture these characteristics, the first step is to identify individual tree crowns from the canopy height model. This is necessary because all further measurements are made at the crown level.

For each crown, four structural variables are calculated:

- Tree height (H)
- Crown diameter (C)
- Height growth (G)
- Crown flatness (F)

These variables are commonly linked to ageing Scots pine. As trees grow old, height growth slows down, crowns expand sideways, and crown shape becomes flatter and less conical (Linder, 1998; Saarinen et al., 2022; Huo et al., 2023). Old-like trees are therefore expected to show specific combinations of these characteristics rather than extreme values in a single variable. To identify such combinations, the analysis focuses on how the four variables occur together. Combinations that appear more often than expected among a small subset of trees are interpreted as potential indicators of old-like structure.

Because tree structure is influenced by growing conditions, the analysis is carried out within site-based strata, defined by elevation, soil moisture and peat depth. This means that, with the help of LIFT, trees are only compared to other trees growing under similar conditions. This reduces variation caused by site productivity and helps isolate structural differences that are more likely related to ageing rather than the environment. This approach follows recommendations from previous ALS studies that emphasize the importance of accounting for ecological site differences when interpreting canopy metrics (Valbuena, 2014; Bonnet et al., 2015).

3. Data and Study Areas

To ensure that the method can be applied in other areas, only national datasets that are widely available to forest stakeholders were used. This avoids reliance on local or specially collected data and allows the workflow to be applied in a similar way across different landscapes. The data summary is presented in Table 2.

Table 2: Data summary of all datasets used in the study, including source, resolution, year and purpose.

Dataset	Source	Resolution	Year	Purpose in Study
1st CHM	Skogforsk	1x1 m	2014	Crown metrics
2nd CHM	Skogforsk (Also openly available via Lantmäteriet)	1x1 m	2022	Crown metrics, crown segmentation
DEM	Lantmäteriet	2x2 m	2019	Stratification, elevation classes
Soil Moisture Index	SLU	2x2 m	2021	Stratification, moisture class
Peat-Depth Model	SLU	2x2 m	2022	Stratification, peat depth class
Protected Areas	Naturvårdsverket	Vector	2025	Desktop validation
Field Inventory Data	Author	GNSS Point	2025	Field validation

3.1 Study Areas

The following subsections provide an overview of the two forest landscapes used in this study. Idre–Särna is the development area where the method was constructed, parameterized and evaluated in detail. Lunsen–Kungshamn–Morga serves as an independent landscape for external validation. Describing both areas ensures that differences in forest structure, management history and site conditions are clearly understood before presenting the results.

3.1.1 Idre–Särna (Development Area)

The primary study area is located between the towns of Idre and Särna in northern Dalarna. This is within the forest holdings of Bergvik Öst, who manages the forest and have long-term experience of the area. According to their management records, the landscape contains a high occurrence of Scots pine, which makes it suitable for developing a method that focuses on detecting old-like structural features. The site is approximately 4 650 hectares within the boundaries presented in Table 3 and Figure 1.

Table 3: Extent for the validation area in Idre–Särna, shown in SWEREF 99 TM and WGS 84.

Corner	SWEREF 99 TM (EPSG:3006)		WGS 84 (EPSG:4326)	
	Easting (m)	Northing (m)	Longitude (°E)	Northing (°N)
NW	389 691	6 855 921	12.906025	61.820144
NE	399 328	9 855 592	13.088842	61.822809
SE	399 328	6 844 113	13.095405	61.716868
SW	389 691	6 844 113	12.913215	61.714215

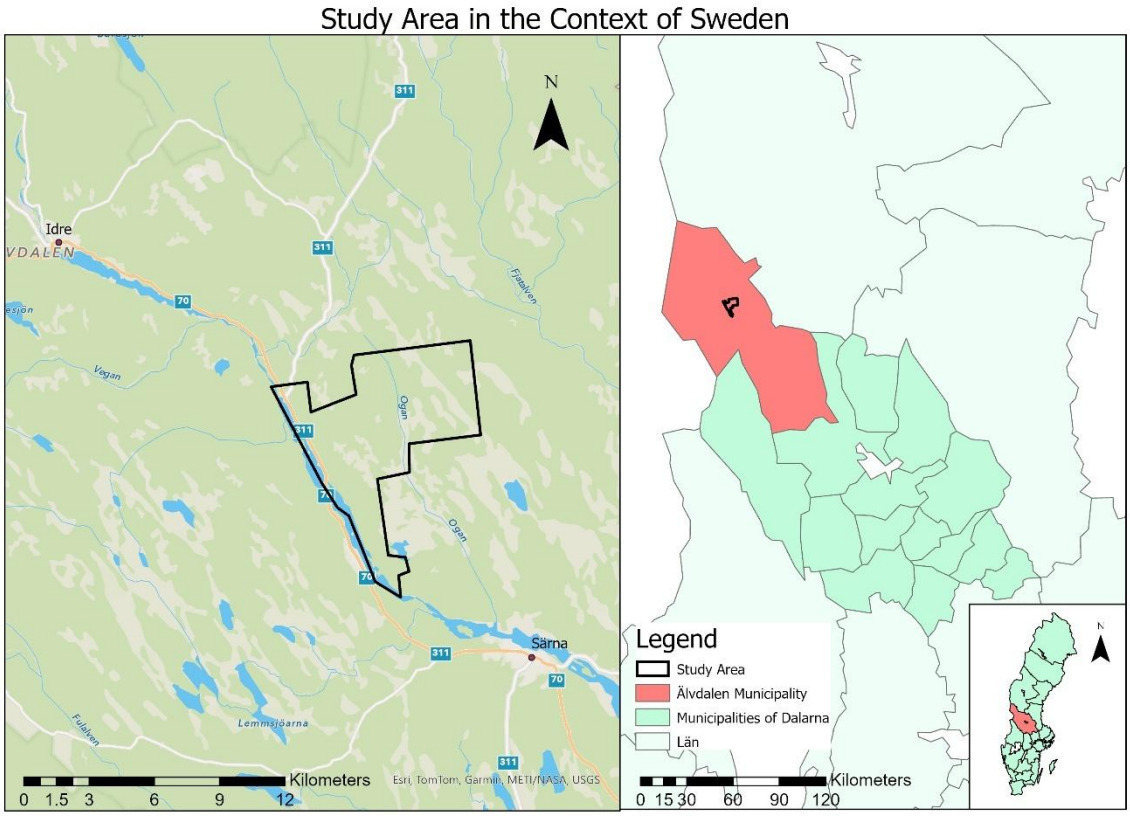

Figure 1: Map of the validation area in Dalarna, with a visual border of the study area and its location in the context of Sweden. © Esri, TomTom, Garmin, FAO, NOAA, USGS, © OpenStreetMap contributors, and the GIS User Community.

Because the area consists largely of older Scots pine, it is also well known for its high conservation value. The forests in the area are mixed with more managed pine stands, making it difficult to identify older trees in advance when planning forestry or conservation work. This creates a practical challenge where planners often know that valuable trees are present, but not exactly where they are or how many there is. These factors makes the area particularly useful for the study and highlights the need for a method that aids field trips.

3.1.2 Southern Lunsen and Kungshamn-Morga (Validation Area)

In order to validate the method, an area consisting of Kungshamn-Morga and southern Lunsen was chosen due to the known occurrence of older Scots pine while also being easily travelled to. The area is located south of Uppsala and lies within both Uppsala- and Knivsta Municipality, covering approximately 2 250 hectares within the boundaries presented in Table 4 and Figure 2.

Table 4: Extent for the validation area in Uppsala-Knivsta, shown in SWEREF 99 TM and WGS 84.

Corner	SWEREF 99 TM (EPSG:3006)		WGS 84 (EPSG:4326)	
	Easting (m)	Northing (m)	Longitude (°E)	Northing (°N)
NW	647 600	6 631 000	17.630062	59.790425
NE	652 000	6 631 000	17.708364	59.788835
SE	652 000	6 626 000	17.704732	59.743987
SW	647 600	6 626 000	17.626535	59.745574

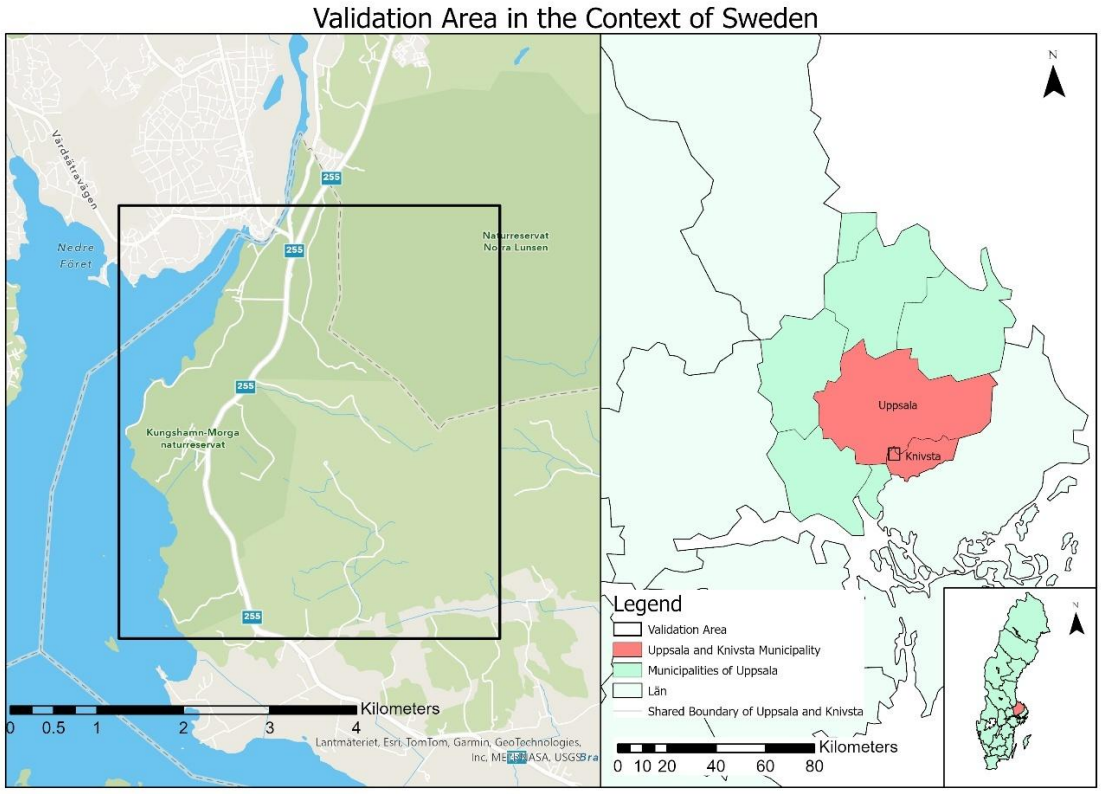

Figure 2: Map of the validation area south of Uppsala, with a visual border of the study area and its location in the context of Sweden. © Esri, TomTom, Garmin, FAO, NOAA, USGS, © OpenStreetMap contributors, and the GIS User Community.

The pines located in Lunsen–Kungshamn–Morga appear in a different landscape setting compared to Idre–Särna, with Lunsen–Kungshamn–Morga containing more recreational forests, less wetland and long-protected nature reserves. This makes the area suitable for external validation of the method, as it differs in general usage and management history. It is also a good test to see how well the method transfers to new site conditions. The site also allowed for an independent evaluation of the model and supported a small field validation, providing a hint of how well the model performed.

3.2 Remote Sensing Data

This section introduces the remote sensing datasets used to derive crown- and canopy-level structural information. The focus is on the national ALS campaigns, which provide the temporal and spatial foundation for tree-level metric calculation and growth assessment.

Although the data originate from national ALS, the analysis in this study does not use raw ALS point clouds. Instead, all processing is based on rasterized canopy height models (CHMs) derived from ALS and provided as standard forest products.

3.2.1 ALS Epochs

This study used two tree height raster datasets derived from the national airborne laser scanning program. The datasets are published by the Swedish Forest Agency (Skogsstyrelsen) as part of *Skogliga Grunddata* (Basic Forest Data) and are based on ALS scans collected by Lantmäteriet (Skogsstyrelsen, 2025).

In the Idre–Särna area, the first dataset is based on ALS data collected in mid-2014 and the second data collected in mid-2022. In the Lunsen–Kungshamn–Morga area, the corresponding datasets are based on ALS data from mid-2011 and early-2021 (Skogsstyrelsen, 2024). The underlying ALS campaigns had average point densities of approximately 0.8 points/m² for the earlier scans and about 1 point/m² for the later scans.

For each epoch, Skogsstyrelsen provides a canopy height model, representing vegetation height above ground. These CHMs were used directly in this study. The most recent CHM in each study area was used to segment individual tree crowns, while both epochs were used to estimate height growth between scans.

3.2.2 Canopy Height Models

The CHMs were the basis of all measurements used in the study. The older CHM is normally only available through the Geodatasamverkan (The Geodata Collaboration) but was made accessible for the study areas by Skogforsk (personal communication, 2025). The newer CHM is openly available, and it served as the main dataset for extracting crown-level structural information (Skogsstyrelsen, 2025).

Each CHM had a 1 x 1-meter resolution and were masked to fit the area of interest, making sure no canopies outside the study area affected the results of the analysis.

3.2.2.1 Derived Canopy Metrics

To describe the structure of individual trees, four canopy metrics were calculated from the segmented crown polygons. The polygons were produced using a watershed-based crown segmentation method applied to the CHM (see 4.1 Crown Segmentation). This step separates the CHM into individual crowns and makes it possible to analyse each tree separately.

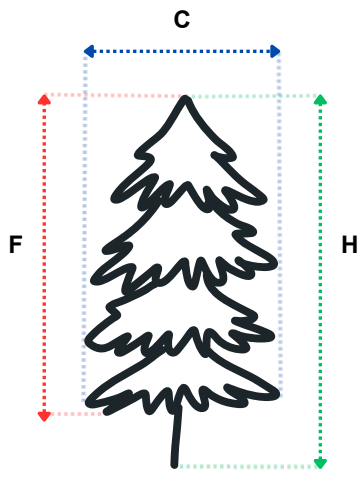

Figure 3: Illustration of three canopy metrics used in this study: crown flatness (F), crown width (C), and tree height (H). The fourth canopy metric growth (G) is not visible in the static image.

From these polygons, four metrics were extracted: tree height (H), crown diameter (C), crown flatness (F) and height growth (G). These variables describe both the shape and development of each tree and were chosen because they are expected to relate to structural ageing (Saarinen et

al., 2022; Huo et al., 2023). The structural metrics are summarized in Table 5 and illustrated in Figure 3. Height growth is based on the difference between the two ALS epochs and is not shown in the static visualization.

Table 5: Overview of the four canopy metrics utilized in the study: Height (H), height growth (G), crown diameter (C), and crown flatness (F).

Metric	Symbol	Unit	Derivation	Ecological Interpretation	Source
P95 Canopy Height	H	m	95th percentile of ALS height within each crown polygon	Indicates long-term canopy dominance; taller crowns typically represent mature individuals	Huo et al., 2023
Height growth	G	m	Difference in the 95th percentile height between omdrev 1 and omdrev 2, divided by time interval	Represents recent vertical growth rate; reduced values indicate slower apical growth typical of ageing trees	Saarinen et al., 2022; Huo et al., 2023
Crown diameter	C	m/year	Horizontal diameter of crown polygon derived from segmentation geometry	Reflects lateral crown expansion and morphological maturity associated with older trees	Kozniewski et al., 2022
Crown flatness	F	m	Difference between the max- and mean crown height	Quantifies crown shape; higher ratios reflect flattened crowns often found in older or suppressed trees	Saarinen et al., 2022; Huo et al., 2023

3.3 Auxiliary Geospatial Data

In addition to the remote sensing data, several other datasets were used to describe the site conditions and build the site-based strata. These datasets provide important background information that helps explain differences in tree growth and crown shape, while also being good at defining stratum boundaries. The following sections briefly describe where each dataset comes from, its resolution and why it was included in the stratification.

3.3.1 Digital Elevation Model (DEM)

A 2 x 2 m Digital Elevation Model (DEM) was downloaded on October 10th, 2025. The DEM was originally produced by Lantmäteriet and was used as the terrain reference for normalizing tree heights and for creating the elevation classes used in the strata. Elevation was divided into three relative classes (low, medium and high) based on percentiles within each study area. The dataset is relatively recent (2019), ensuring good elevation detail for the study area (Lantmäteriet, 2019).

3.3.2 Soil Moisture Data

Soil moisture was described using the SLU *Markfuktighetskarta* v1.0, a national 2 x 2 m raster that shows relative wetness across Sweden (SLU, 2020). The map was produced by modelling terrain from Lantmäteriet's elevation data (2019) together with field plots from the Swedish National Forest Inventory. The methodology behind it is presented in Ågren et al. (2021).

The product contains two layers:

1. A continuous index from 0 (dry) to 100 (wet)
2. A classified map with four soil-moisture classes: dry-fresh, fresh-moist, moist-wet and water.

In this study, the classified layer was used because it provides ecological categories that are interpretable and directly usable. The classes reflect clear differences in soil conditions, which is later used for building the site-based strata and dividing the area into smaller groups. This means that four different soil moisture classes are used for the stratification.

3.3.3 Peat Depth Data

Peat depth was described using a national peat map developed by SLU (Ågren et al., 2022). The map shows where soils are mineral or peat-based and was created by combining ALS-derived terrain data, a national soil-moisture map and measurements of organic layer thickness from 5 479 field plots across Sweden. The product includes both continuous and classified layers, where peat soils are grouped into depth classes of ≥ 30 cm, ≥ 40 cm and ≥ 50 cm. The method performed well when tested against independent field data and was able to detect smaller peat areas.

In this study, the classified peat map was used to assign each tree crown to one of five peat-depth classes: water, mineral soil, peat ≥ 30 cm, peat ≥ 40 cm, peat ≥ 50 cm, which means that five total peat depth classes were used for the stratification.

3.3.4 Protected Areas

The boundaries for protected areas were obtained from Naturvårdsverket's national dataset *Skyddade områden: naturreservat (Protected areas: nature reserves),* which provides official polygons for all nature reserves and national parks in Sweden (Naturvårdsverket, 2025). These areas were used to identify forests where structure and age are expected to differ from the surrounding managed landscape. In this study, protected areas are used as a form of desktop validation, under the assumption that long-protected forests are more likely to contain structurally old trees than surrounding managed forests.

In the Lunsen–Kungshamn–Morga region, three nature reserves are relevant: Kungshamn–Morga (established 1963), Northern Lunsen (2003) and Southern Lunsen (2020) (Länsstyrelsen Uppsala, n.d.-a; n.d.-b; n.d.-c.). For the desktop validation, only the Kungshamn–Morga reserve was used because it has been protected for the longest time and contains well-known stands of older Scots pine. Its long and continuous protection means that the forest structure reflects minimal management, making it a suitable reference area for evaluating the model's predictions.

4. Method

This study followed a structured, three-phase analytical framework:

1. Data preparation and crown segmentation.
2. Site-based stratification
3. Adaptive LIFT-based threshold analysis

An overview of the entire workflow is presented in Figure 4 and is also available in appendix D.

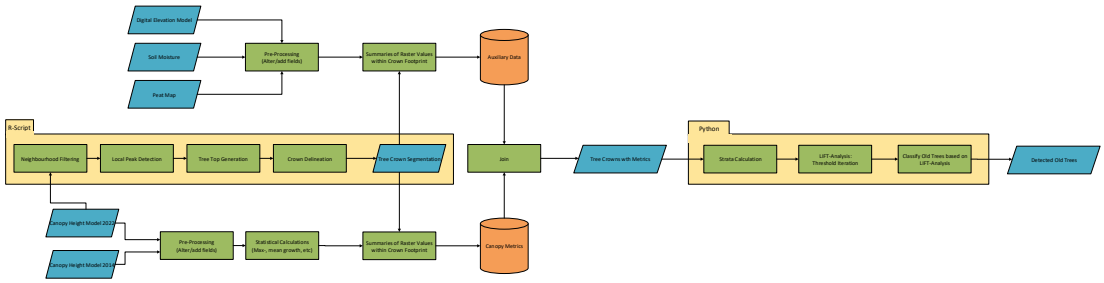

Figure 4: Overview of the methodological workflow, with blue standing for input/output, green for process and orange for a group of datasets.

All spatial steps in the analysis were carried out in a geographic information system (GIS) and scripted in Python. The crown segmentation was carried out in R. The workflow was divided into four main parts: crown segmentation, site-based stratification, threshold search and final classification. The aim of this structure is to make the process easy to follow and reproduce. The methods are described in general terms so they can be replicated in any GIS/Python setup. ArcGIS Pro was used in this study, but the approach does not rely on software-specific tools.

All Python and R scripts used in the analysis are available in a public GitHub repository (SimWest2001, 2025), which allows full reproducibility.

4.1 Crown Segmentation

Tree crowns were segmented from the latest canopy height model and used as the base unit for all measurements in the study. The segmentation was carried out in R using the ForestTools and terra packages. These packages were chosen because they are flexible, open-source and well documented, which makes the workflow easy to reproduce (Plowright, 2023; Hijmans, 2023).

Before segmentation, the CHM was smoothed with a small 3 x 3 mean filter to smooth out small height variations, reducing noise and the risk of over-segmenting. After smoothing, local maxima were detected using two circular window sizes: a larger window, ranging from approximately 1.0 to 2.5 m, to find the main treetops, and a smaller window, approximately 0.8 to 1.8 m, to capture additional peaks inside dense stands. The combined maxima were used as markers for a marker-controlled watershed segmentation. During crown segmentation, CHM cells with heights below 3 meters were excluded by the segmentation algorithm and were therefore not allowed to contribute to crown segmentation. This prevented low vegetation and shrubs from being included in tree crowns while keeping the original CHM unchanged. The marker-controlled watershed segmentation was implemented using the *mcws* algorithm in ForestTools package. In this step, the inverted CHM surface was segmented by expanding regions outward from each treetop until crown boundaries met a local height minima, resulting in individual tree crown polygons (Plowright, 2023). This two-step approach helps each polygon represent a single tree crown while reducing cases where several trees merged or a tree is split into multiple parts. The parameters were adjusted through visual checks until crown shapes matched the height patterns in the CHM.

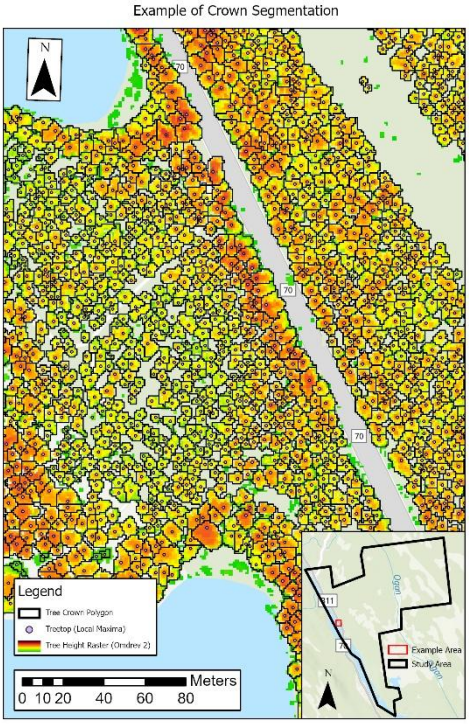

Figure 5: An example of the crown segmentation visualized in the development area of Idre–Särna. Every polygon represents an individual tree. © Esri, TomTom, Garmin, FAO, NOAA, USGS, © OpenStreetMap contributors, and the GIS User Community

The final crown polygons served as the basis for all canopy metrics and later statistical analyses. A small example of the segmentation is shown in Figure 5, and Figure 6 displays how the polygons align with the 2022 orthophoto (Lantmäteriet, 2024b).

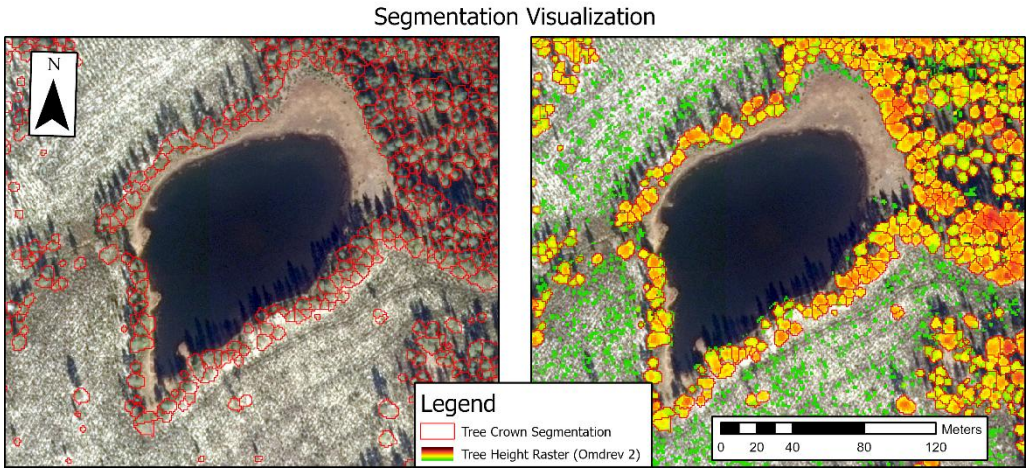

Figure 6: Comparison between segmented crowns in an orthophoto and the canopy height model, side-by-side. © Lantmäteriet.

4.2 Site-Based Stratification

To account for differences in site conditions, each segmented crown was assigned three environmental variables: elevation, soil moisture and peat depth. These variables influence how Scots pine grow and how structural ageing is expressed. Using them allowed crowns to be grouped into site-based strata that capture local variation in growing conditions.

Elevation was derived from the DEM and divided into three classes (low, medium and high) based on percentiles (Lantmäteriet, 2019). Soil moisture class came from the SLU soil-moisture map, which separates dry-fresh, fresh-moist, moist-wet and water sites (SLU, 2020; Ågren et al., 2021). Peat depth was taken from the national peat map, which separates water, mineral soil and peat layers deeper than 30, 40 or 50 cm (Ågren et al., 2022).

Not all combinations of these variables exist in the landscape, but the grouping helps reduce the effect of environmental variation when comparing crown structures. It is important to note that this stratification does not control for stand age. Some groups may still contain trees of different ages, which can influence height and growth patterns. No age filtering was applied before stratification, so the results should be interpreted with this in mind.

4.2.1 Assignment of Ecological Strata

The ecological variables described above were added to each crown polygon using a rule-based overlay. Before this step, all layers (raster) were clipped to the study area. This ensured that the layers matched each other and that crowns were compared against the correct underlying terrain and soil information.

For elevation, all raster cells inside each tree crown polygon were averaged, with the mean value then being assigned to each respective crown. Using the mean value avoids giving too much weight to a single high or low cell and gives a stable estimate of the terrain position under the whole crown.

For soil moisture and peat depth, each crown was assigned the class that covered most of its footprint. This majority approach captures the dominant condition under the tree while still

handling crowns that cross class boundaries. However, the soil- and peat maps are not perfect, and local inaccuracies can occur near class edges. The majority rule therefore provides a simple and consistent way to assign each crown to one main class.

After the classification, all variables were standardized and numeric classes were converted into clear text labels (e.g., 1 = “dry-fresh”, 2 = “fresh-moist” etc.). This ensured that the stratification and the later analysis were easy to interpret and apply.

4.3 LIFT-Based Candidate Evaluation

The LIFT analysis was implemented as a scripted workflow operating on crown-level data within each stratum, with a simple visualization present in Figure 7 as well as in appendix D.

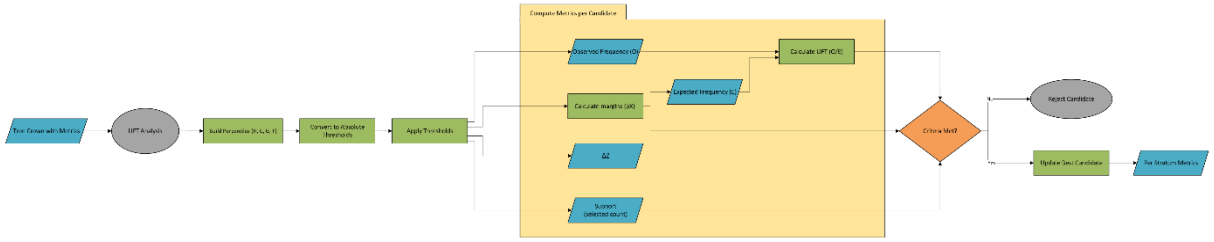

Figure 7: Schematic view of the LIFT-analysis, which calculates a LIFT value for every threshold combination.

Every candidate rule is defined by thresholds for height, height growth, crown diameter and crown flatness, and for every candidate rule, the algorithm calculates observed and expected prevalence. This allows it to also calculate the LIFT value that is the deciding factor for a structurally old tree.

To ensure stability, three quality filters were applied. The filters were selected to reduce the influence of small sample sizes, random co-occurrence, and extreme outliers. Prioritizing robust and interpretable structural patterns rather than exhaustive detection:

- Minimum LIFT: A minimum LIFT value of 2.0 is required.
- Minimum ΔZ: A minimum of 0.3 standard deviations is required.
- Minimum support: There must be at least 30 crowns per stratum.

ΔZ measures how strongly the observed prevalence deviates from the expected prevalence, expressed in standard deviations. This filter ensures that enriched patterns represent a meaningful structural signal rather than minor statistical fluctuations. All three quality filters are fully adjustable depending on what the algorithm should look for as well as what the landscape looks like. An example of how LIFT works is presented in appendix E.

4.3.1 Grid Search

A grid search procedure was used to systematically test many combinations of percentile-based thresholds for the four canopy metrics. Instead of using fixed or arbitrary cut-off values, this approach evaluates many possible threshold combinations to find those that best separate old-like crowns from the rest.

For each stratum, percentile thresholds were generated directly from the distribution of trees within that stratum. This means that all threshold testing was done among trees growing under

similar conditions, rather than across the entire study area. Each variable was tested at several percentile steps, and together these steps formed a grid of possible threshold combinations. Each point in the grid presented one candidate rule, for example:

$$H \geq P90;\ G \leq P40;\ C \geq P85;\ F \leq P95$$

Each structural metric (height, growth, crown diameter and crown flatness) was tested at a predefined number of percentile levels. Together, these define the grid density and decides how fine the search is. In this study, each variable was tested at seven percentile steps, resulting in:

$$7\ x\ 7\ x\ 7\ x\ 7 = 2\ 401 \qquad \text{Equation 4}$$

2 401 candidate threshold combinations per stratum. Denser grids can be used if a more exhaustive search is required. For example, testing ten percentiles per variable increases the search space to 10 000 combinations, which comes at the cost of higher computational demand.

For every candidate rule, the algorithm calculates LIFT, support and effect size (ΔZ). The grid search then selects the rule that maximizes LIFT while still meeting the quality filters presented previously. Maximizing LIFT ensures that the selected threshold combination represents the strongest deviation from random co-occurrence. This means that the associated canopy traits appear together far more often than expected by chance. In this context, the rule with the highest valid LIFT is interpreted as the most distinctive and structurally meaningful pattern within the stratum, and therefore the best-performing threshold.

4.3.2 Threshold Selection and Output

For each stratum, the grid search returned one optimal candidate rule, defined by the threshold values for the structural metrics. Each crown was checked against the candidate rule identified by the grid search. If it met all of the criteria, the crown was assigned “is_old” = 1, indicating old-like structural characteristics. Crowns that did not meet all thresholds were assigned “is_old” = 0. In strata where no rule passed the quality filters, no crowns were classified as old-like.

The classification results were written to the crown attributes. This made it possible to map the predicted old-like crowns and summarize them together with the other structural and site variables.

4.4 Validation and Field Verification

To verify that the thresholding approach identifies old-like pines rather than random trees, two types of validations were performed: a desktop validation and a smaller field validation. These assessments provide a first indication of the method’s performance and ecological relevance.

4.4.1 Desktop Validation

The desktop validation checks whether the ALS-based classification behaves in a reasonable ecological way, without relying on field data. The basic idea is that long-protected forests usually contain older and less intensively managed trees than the surrounding landscape. If the

classifier is meaningful, predicted old-like crowns should appear more often inside a protected area than outside it.

All classified crowns in the Lunsen–Kungshamn–Morga region were intersected with the protected area polygons from the Swedish Environmental Protection Agency (Naturvårdsverket, 2025). Because Kungshamn–Morga has been protected since 1963, it was used as the main reference area for this validation. The assumption is not that the reserve contains only old trees, but that it provides a useful structural contrast to the surrounding forest.

Each crown was marked as either inside or outside the reserve. This made it possible to calculate:

The proportion of predicted old-like crowns occurring inside the protected area:

$$P(Protected\ |is\_old = 1) = \frac{n_{old \cap Protected}}{n_{old \cap Protected} + n_{old \cap Unprotected}} \quad \text{Equation 5}$$

The proportion of predict non-old like crowns inside the protected area:

$$P(Protected\ |is\_old = 0) = \frac{n_{non-old \cap Protected}}{n_{non-old \cap Protected} + n_{non-old \cap Unprotected}} \quad \text{Equation 6}$$

An enrichment ratio (ER) was then computed as:

$$ER = \frac{P(Protected\ |is\_old=1)}{P(Protected\ |is\_old=0)} \quad \text{Equation 7}$$

ER expresses how many times more common the predicted old-like crowns are inside the reserve compared to what would be expected from the distribution of all other crowns. This is a simple use-availability comparison (Manly et al., 2002). If the value is higher than 1, old-like crowns appear in the reserve more often than expected by chance. If it is close to 1, the classified is not distinguishing the reserve from the surrounding forest.

Conceptually, the enrichment ratio mirrors the role of LIFT in the threshold search. Both measure whether something appears more often than expected under a baseline assumption, but in different contexts. LIFT is used in canopy-metric space and ER in geographic space.

4.4.2 Field Validation

The field validation tests how well the ALS-based classification (is_old = 1) matches real old Scots pine individuals in the forest. A small but structured sample was collected during a field visit in late November.

For every crown predicted as old-like, the corresponding tree was first identified and assessed in the field. In addition, two comparison trees were selected:

1. Nearest Scots pine that is not predicted as old-like (to test possible false negatives)
2. A Scots pine ≈ 30 m away in a southward direction (to provide an additional control tree under similar site conditions)

This resulted in groups of three field-assessed trees per predicted crown, consisting of one predicted and two unpredicted individuals located close to each other. This approach made it possible evaluate both correct and incorrect model predictions under comparable conditions.

Tree locations were collected with a mobile mapping app and an Eos Arrow 100 GNSS receiver mounted on a 2-meter pole. The arrow receiver was used because it gives sub-meter accuracy, which made it possible to match each field tree to the right segmented crown.

For every visited pine, we recorded structural features linked to age following the Swedish Forest Agency's protocol "*Levande träd och buskar med naturvärden" (Living trees and bushed with ecological values)*. Examples include bark texture, dead branches, diameter at breast height, fire scars and crown shape (Skogsstyrelsen, n.d.). Based on these traits, each tree was classified in the field as old or not old. The field inventory form can be found in appendix C.

After the field work, each observation was joined to the crown polygons using its GNSS position. This allowed a direct comparison between what the model predicted and what was observed in the field. From this comparison, precision, recall and the F1-score was calculated:

$$Precision = \frac{TP}{TP+FP} \quad \text{Equation 8}$$

$$Recall = \frac{TP}{FP+FN} \quad \text{Equation 9}$$

$$F1 = 2 * \frac{Precision * Recall}{Precision + Recall} \quad \text{Equation 10}$$

The four metrics used in the formulas are:

- True Positive (TP): model predicts old-like, and the tree is old in the field.
- False Positive (FP): model predicts old-like, and the tree is not old in the field.
- True Negative (TN): model predicts not old, and the tree is not old in the field.
- False Negative (FN): model predict not old, but the tree is old in the field.

Precision shows the fraction of predicted old trees that were confirmed as old in the field. Recall shows the fraction of field-identified old trees that were correctly detected by the model. The F1-score combines both into one number and is more informative than overall accuracy when the target class is rare (Manning, et al., 2009).

5. Results

The results are presented in two parts. First, the method is applied in the development area of Idre–Särna, where all components were tested. Second, the method is evaluated in the independent landscape of Lunsen–Kungshamn–Morga. This structure reflects the workflow in the methods chapter.

5.1 Idre–Särna

5.1.1 Segmentation and Descriptive Statistics

The crown segmentation produced 726 763 individual tree crowns in the Idre–Särna area. The resulting canopy metrics showed clear structural variation across the landscape (Table 6). Crown height (H) had a median of 11.7 m, ranging from 3.4 to 30.6 m. Annual height growth (G) had a median of 0.21 m/year, with a wide range where some extreme values occurred, reflecting some value errors in the CHMs (Figure 8). Median crown diameter (C) was 6.18 m, with values between 2.76 and 17.15 m. Crow flatness (F) ranged from near 0 to 15.75 m, with a median of 3.76 m, indicating notable variation in vertical crown shape.

Table 6: Tree crown metrics across the validation area of Idre–Särna.

Variable	Minimum	Maximum	Mean	Median	Standard Deviation
H (m)	3.40	30.60	11.77	11.70	4.05
G (m / year)	-4.99	2.23	0.23	0.21	0.18
C (m)	2.76	17.15	6.18	6.18	1.59
F (m)	0.00	15.75	3.88	3.76	1.86

The value error in Figure 8 originates from the ALS dataset from 2014, where the two black raster cells contain no-data values. When height growth was calculated between the two epochs, these no-data cells resulted in unrealistic growth values for a very small number of crowns. These extreme values does not represent true biological growth.

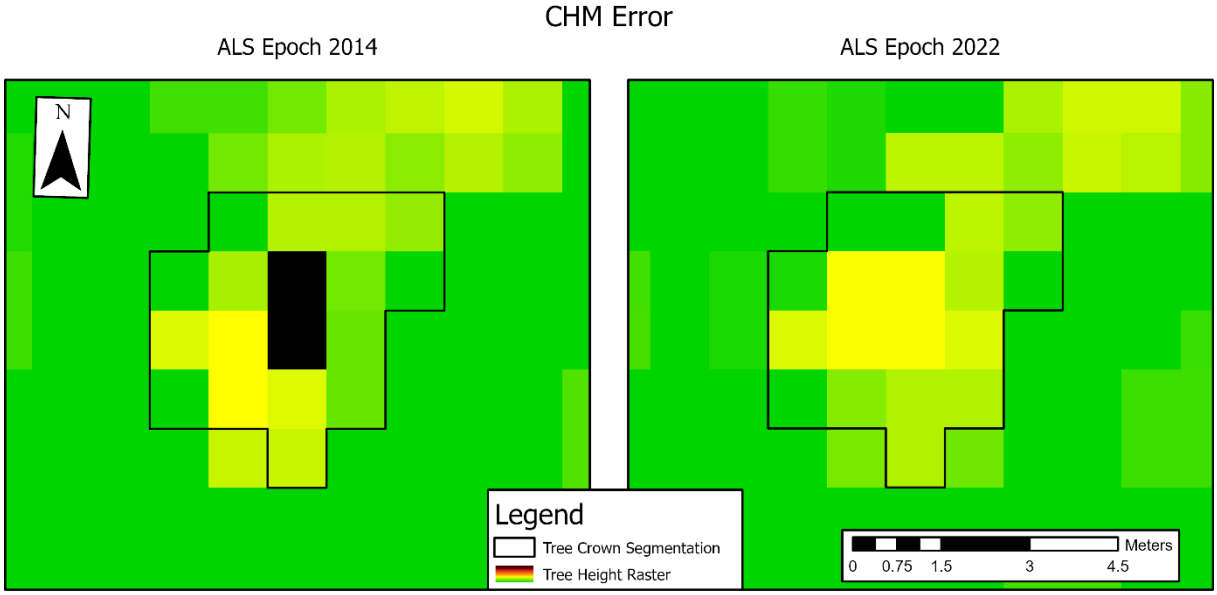

Figure 8: Example of a value error in the canopy height model, where extreme values are the results of the error.

Figure 9 illustrates the segmentation across the study area. Areas without trees appear as gaps, consistent with clearcuts and other open terrain.

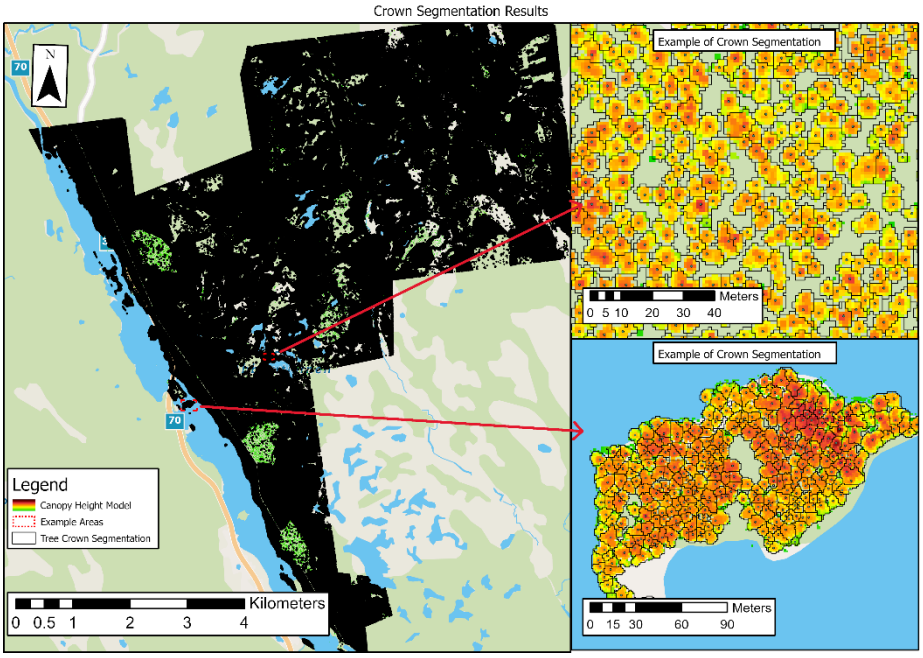

Figure 9: Visualization of the 726 763 individual tree crowns in the development area of Idre–Särna. Two examples of crown areas are visualized, one is a semi-empty area, and one is a small island the water to west of the area. © Esri, TomTom, Garmin, FAO, NOAA, USGS, © OpenStreetMap contributors, and the GIS User Community.

5.1.2 Stratification Overview

The stratification defined 38 possible site-based strata, based on elevation, soil moisture and peat depth. 726 689 crowns fell into one of the realized strata, whereas the remaining 74 crowns consisted of fragmented polygons along edges and could therefore not be assigned a stratum.

The number of crowns per stratum varied widely. The largest stratum was low elevation, dry-fresh, mineral soil sites and contained more than 240 000 crowns, while rare combinations (e.g., dry-fresh sites with deep peat) sometimes contained fewer than ten crowns. Most crowns were concentrated in mineral-soil strata across all elevation bands, whereas strata involving water surfaces, very wet soils or deep peat frequently contained fewer than a couple of hundred crowns.

A complete list of stratum-level statistics is provided in appendix A.

5.1.3 LIFT-Based Threshold Identification

The LIFT evaluation was applied to all strata. Of the 38 strata present in the study area, 14 produced at least one threshold combination that passed all quality filters and were therefore considered stable. These strata are presented in Table 7 and had all sufficiently large sample sizes, ranging from approximately 5000 to 240 000 crowns per stratum. Across the strata with valid results, LIFT values ranged from 2.3 to 12.7, indicating that the selected combinations of canopy metrics occurred between roughly two and thirteen times more often than expected.

The strongest enrichment signals were consistently found in dry-fresh, mineral soil strata across all elevation classes. Fresh-moist strata on mineral or shallow peat soils also produced valid threshold combinations, although with generally lower LIFT values. Strata associated with moist-wet conditions or deeper peat did not produce threshold combinations that passed all quality filters.

Across the retained strata, the selected percentile thresholds showed consistent patterns. Crown flatness thresholds (F) were consistently in the 95th percentile, which was the highest value allowed. Crown diameter thresholds (C) were also high, commonly exceeding the 90th percentile. Height (H) thresholds varied more between strata, while height growth (G) were consistently located in the lower part of the distribution.

Table 7: List of strata that gave stable LIFT values (>2), which means a threshold combination is identified that indicates structurally old trees in Idre–Särna.

						Threshold in Percentiles			
Elevation	**Soil Moisture**	**Peat Depth**	**LIFT**	**Sample size**	**ΔZ**	**H**	**G**	**C**	**F**
H	Fresh-Moist	≥ 30 cm	5.3	8714	1.02	86.9	42.8	99.0	95.0
H	Fresh-Moist	≥ 40 cm	2.7	5594	0.82	81.5	47.7	93.5	95.0
H	Fresh-Moist	≥ 50 cm	2.8	11929	1.65	90.7	68.2	98.9	95.0
H	Fresh-Moist	Mineral soil	5.9	17724	1.07	91.9	35.7	98.9	95.0
H	Moist-Wet	≥ 50 cm	2.6	5178	2.71	95.8	87.9	95.7	95.0
H	Dry-Fresh	Mineral soil	12.7	34363	0.79	94.7	21.4	99.0	95.0
M	Fresh-Moist	≥ 30 cm	2.9	15894	0.67	85.8	30.9	94.0	95.0
M	Fresh-Moist	≥ 40 cm	3.4	10133	0.95	89.8	38.6	90.7	95.0
M	Fresh-Moist	≥ 50 cm	2.3	34652	1.19	86.7	54.2	93.9	95.0
M	Fresh-Moist	Mineral soil	3.5	36022	0.91	90.8	33.1	93.6	95.0
M	Dry-Fresh	Mineral soil	7.9	199272	0.53	93.7	15.5	98.9	95.0
L	Fresh-Moist	≥ 30 cm	2.3	10666	0.71	81.7	36.7	92.9	95.0
L	Fresh-Moist	Mineral soil	2.8	27044	0.60	73.9	32.0	99.0	95.0
L	Dry-Fresh	Mineral soil	6.1	243270	0.91	93.8	25.2	98.9	95.0

5.1.4 Classification Output

A total of 1 457 crowns were classified as old-like in Idre–Särna (Figure 10), representing approximately 0.2% of all crowns. The crown distribution across strata are quite even, except for the top 2 strata being low and medium elevation, dry-fresh, mineral soil sites. They represent almost 32% of all crowns.

Most old-like crowns occurred in the same strata that produced the strongest LIFT values, especially dry-fresh, mineral soil. Spatially, the classified crowns appear as both scattered individuals and as small clusters. Very few old-like crowns were predicted in moist or wet areas.

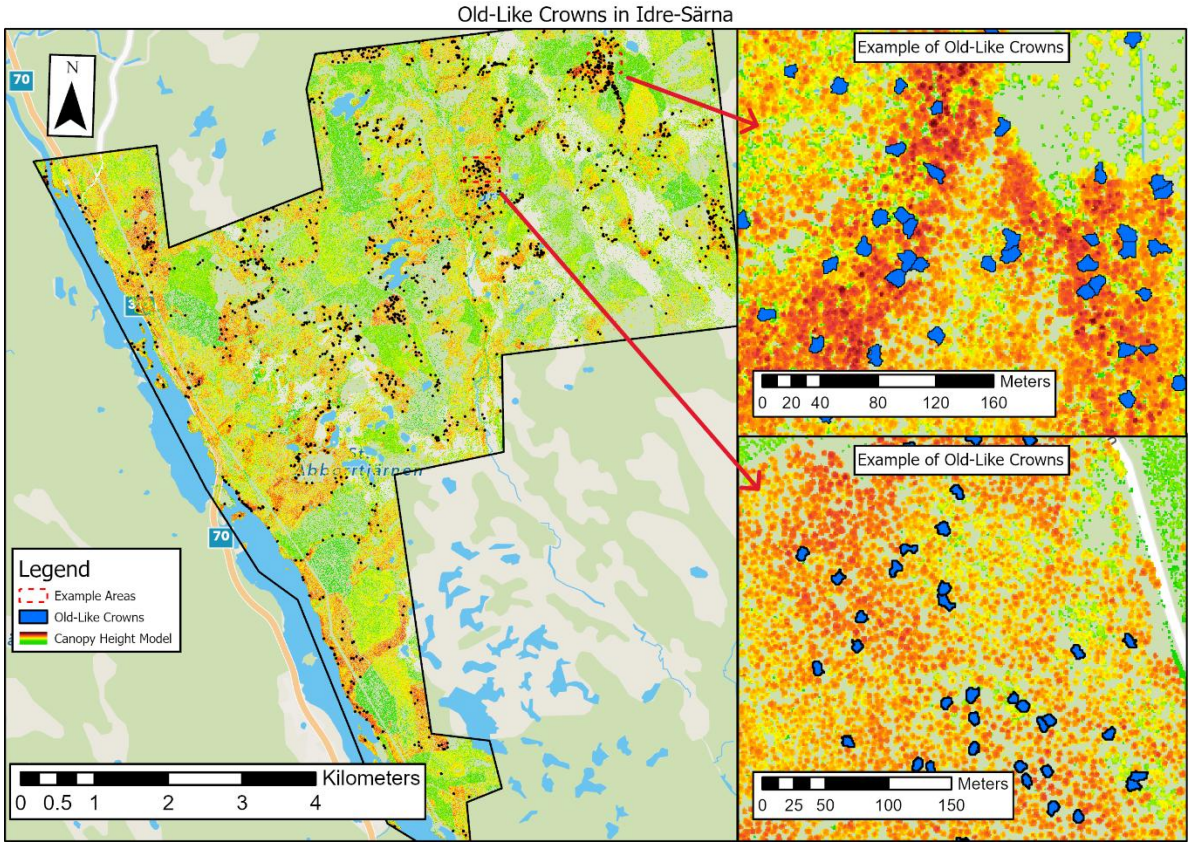

Figure 10: Visualization of the 1 457 crowns classified as old-like in Idre–Särna. Most occur in dry-fresh mineral soils. Two examples of old-like dense areas are visualized further. © Esri, TomTom, Garmin, FAO, NOAA, USGS, © OpenStreetMap contributors, and the GIS User Community.

5.2 Lunsen–Kungshamn–Morga

5.2.1 Segmentation and Stratification

The crown segmentation in Lunsen–Kungshamn–Morga resulted in a total of 314 993 individual crowns. Figure 11 shows the segmentation results for the entire area, along with two detailed examples from different parts of the area. As presented in the study area, the segmented crowns represent a landscape with a different focus compared to Idre–Särna.

The stratification procedure identified a total of 38 site-based strata within the landscape. Most crowns were in strata associated with mineral soils and fresh-moist conditions, while wet or peat-influenced strata contained fewer crowns. This distribution reflects the spatial extent of forested land and the limited presence of water in wetter areas.

Appendix B shows all stratification data for Lunsen–Kungshamn–Morga.

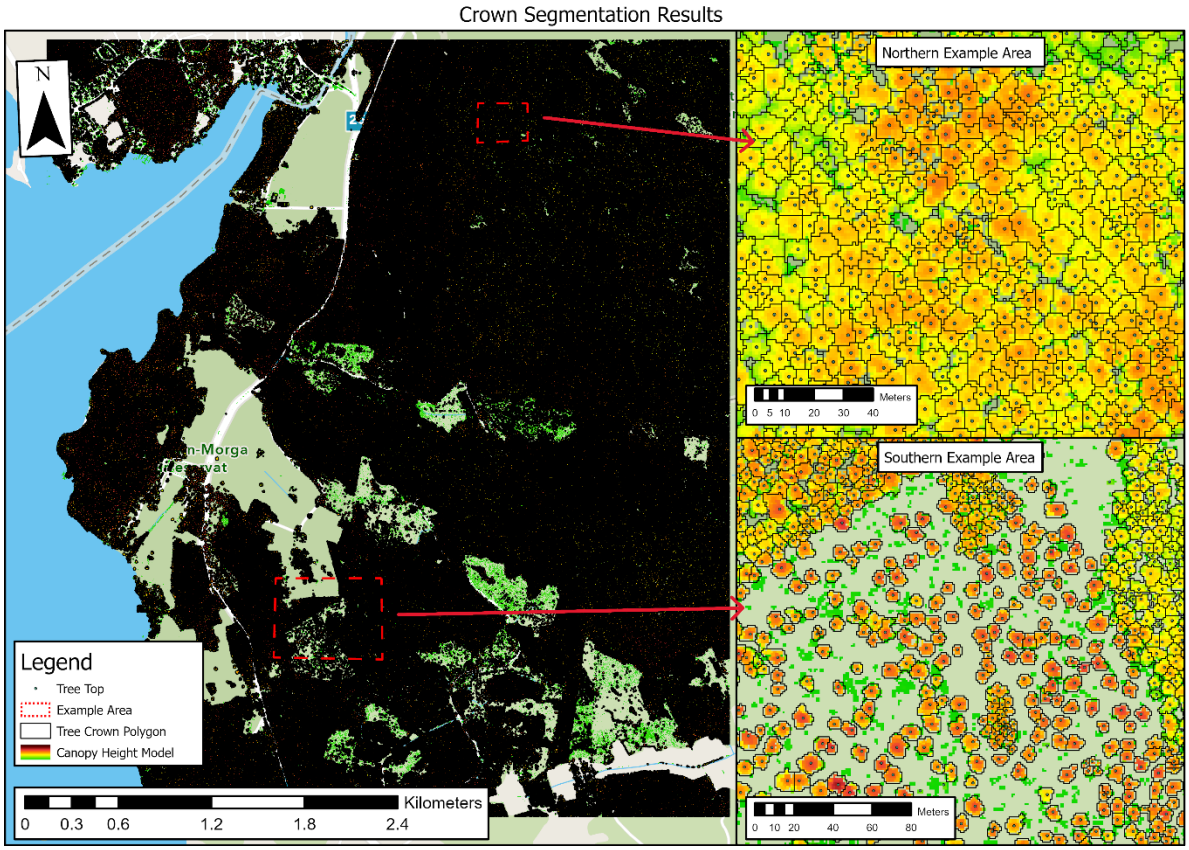

Figure 11: Visualization of the 314 993 individual tree crowns in the validation area of Lunsen–Kungshamn–Morga. Two examples of crown areas are visualized, one is in a tree dense part of the area, and one is sparser. © Esri, TomTom, Garmin, FAO, NOAA, USGS, © OpenStreetMap contributors, and the GIS User Community.

5.2.2 LIFT-Based Threshold Identification

The LIFT evaluation was applied to all site-based strata in the Lunsen–Kungshamn–Morga area. Of the 38 strata, 10 produced at least one threshold combination that passed all quality filters and were therefore retained. These strata are presented in Table 8 together with their corresponding LIFT values, sample sizes, ΔZ, and selected percentile thresholds.

Sample sizes for the strata ranged from 20 to approximately 90 000 crowns. For these strata, LIFT values ranged from 2.2 to 6.7, indicating that the selected combinations of canopy-metrics thresholds occurred between 2 and 7 times more frequently than expected.

Valid threshold combinations were identified across all three elevation classes and several soil moisture and peat depth categories. The highest LIFT values occurred in dry–fresh mineral soil strata, while fresh–moist and moist–wet strata also produced valid results. One valid threshold combination was identified in a water-dominated stratum.

The selected percentile thresholds showed consistent patterns. Crown flatness thresholds (F) were uniformly in the 95th percentile. Crown diameter threshold (C) were generally high, often close to or at the upper percentiles of the distribution. Height thresholds varied between strata, while height growth thresholds were consistently located in the lower part of the distribution.

Table 8: List of strata that gave stable LIFT values (>2), which means a threshold combination is identified that indicates structurally old trees in Lunsen–Kungshamn–Morga.

						Threshold in Percentiles			
Elevation	**Soil Moisture**	**Peat Depth**	**LIFT**	**Sample size**	**ΔZ**	**H**	**G**	**C**	**F**
H	Moist-Wet	Mineral Soil	3.7	20	0.52	62.0	47.4	70.0	95.0
L	Fresh-Moist	≥ 30 cm	2.2	527	0.49	63.7	32.1	92.0	95.0
L	Fresh-Moist	≥ 40 cm	2.5	168	0.47	65.0	29.9	83.0	95.0
L	Fresh-Moist	Mineral Soil	4.4	9084	0.92	85.6	27.3	99.0	95.0
L	Dry-Fresh	Mineral Soil	3.3	89855	0.81	84.6	33.7	99.0	95.0
L	Water	Water	2.2	458	1.73	89.0	58.4	88.0	95.0
M	Fresh-Moist	≥ 50 cm	3.7	1390	0.38	58.5	20.2	99.0	95.0
M	Fresh-Moist	Mineral Soil	2.2	14233	0.83	85.5	16.4	99.0	95.0
M	Moist-Wet	≥ 50 cm	2.4	1045	1.22	93.0	23.9	82.7	95.0
M	Dry-Fresh	Mineral Soil	6.7	86426	1.47	99.0	12.4	99.0	95.0

5.2.3 Classification Output

A total of 211 crowns were classified as old-like in Lunsen–Kungshamn–Morga (Figure 12), representing 0.067% of all crowns. Most classified crowns came from two strata:

- Medium elevation | dry-fresh | mineral soil (87 crowns)
- Low elevation | dry-fresh |mineral soil (67 crowns)

Together, these strata accounted for about 73% of all predicted old-like crowns. Clusters were found both in recreation forests and within the Kungshamn–Morga nature reserve.

These maps formed the basis for the desktop and field validation.

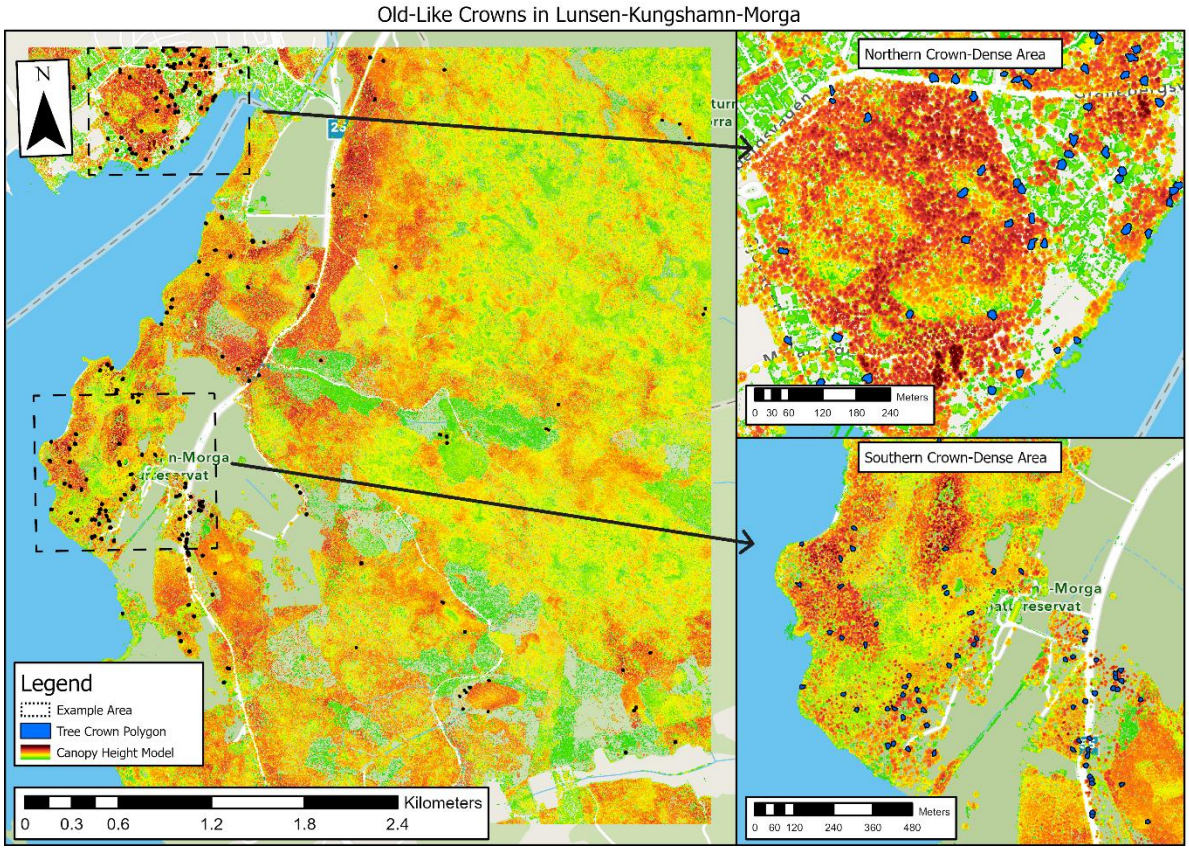

Figure 12: Visualization of the 211 crowns classified as old-like in Lunsen–Kungshamn–Morga. Most occur in dry-fresh mineral soils. Two examples of old-like dense areas are visualized further. © Esri, TomTom, Garmin, FAO, NOAA, USGS, © OpenStreetMap contributors, and the GIS User Community.

5.2.4 Desktop Validation

In total, 113 of 211 old-like crowns (≈ 54%) occurred within the Kungshamn–Morga nature reserve.

$$P(Protected \mid is\_old = 1) = \frac{113}{113+98} \approx 0.536 \qquad \text{Equation 11}$$

$$P(Protected \mid is\_old = 0) = \frac{92\,470}{92\,470+222\,312} \approx 0.294 \qquad \text{Equation 12}$$

$$ER = \frac{0.536}{0.294} \approx 1.82 \qquad \text{Equation 13}$$

This resulted in an enrichment ratio of approximately 1.82, meaning old-like crowns were nearly twice as common inside the long-protected reserve than expected from the distribution of all other crowns. Even though this does not confirm true age of individual trees, it shows that the model highlights trees in places where older forest structures are expected to occur.

5.2.5 Field Validation

A total of 63 trees were visited during the field survey. Field assessments identified 59 trees as old-like and 4 as not old, based on structural indicators.

The comparison with the methods predictions resulted in Table 9.

Table 9: Confusion matrix comparing ALS-based predictions with field-observed age status

	Old In Field	**Not Old In Field**
Predicted Old	TP = 21	FP = 0
Predict not Old	FN = 38	TN = 4

This corresponds to:

$$Precision = \frac{21}{21 + 0} = 1 \quad \text{Equation 13}$$

$$Recall = \frac{21}{21+38} \approx 0.37 \quad \text{Equation 14}$$

$$F1 = 2 * \frac{1 * 0.37}{1 + 0.37} \approx 0.54 \quad \text{Equation 15}$$

The results show that when the model predicts a tree as old-like, it is very reliable. However, it detects only a small amount of all old-like trees, which reflects the thresholds conservative nature. However, it must be noted that crown segmentation errors occasionally caused a mismatch between mapped crowns and individual trees. This must be considered when analysing the results and it will be further discussed in the discussion.

6. Discussion

This thesis aimed to develop and evaluate a method for identifying Scots pine trees with old-like structural characteristics, which was done using nationally available ALS data. The method combines crown-level structural metrics, site-based stratification, and LIFT-based thresholding to detect trees that structurally stand out relative to their local surrounding. The discussion interprets the main findings, evaluates the method performance and limitations, and considers implications for forestry and conservation.

6.1 Structural Signatures of Old-Like Scots Pine

The results show that a combination of canopy height, crown diameter, crown flatness and reduced height growth can capture structural traits commonly associated with ageing Scots pine. These findings agree with established ecological understandings that ageing Scots pine gradually shifts from vertical to lateral growth, developing wider and flatter crowns while height increment declines (Linder, 1998; Saarinen et al., 2022; Huo et al., 2023).

Importantly, no single metric was sufficient to identify old-like trees on its own. Height alone was not a reliable indicator of ageing, particularly in productive stands where many trees achieve large stature at relatively young ages. This supports earlier observations that large trees are not necessarily old, and old trees are not necessarily large (Helms, 2004). Instead, ageing was expressed through combinations of traits, reinforcing the need for a multivariate approach rather than fixed thresholds applied to individual variables.

Across both study areas, the structural niche associated with old-like trees was rare. In most strata, fewer than 1% of crowns met all threshold criteria. This reflects the ecological reality that structurally mature trees form a narrow structural niche within managed forests (Linder, 1998). The rarity of selected trees also explain why strong enrichment values (high LIFT) could occur despite the numbers of selected individuals.

6.2 Influence on Site Conditions and the Role of Stratification

The performance of the method varied across the strata. The strongest and most stable threshold patterns were found in dry-fresh mineral soil strata, while moist, peat-dominated or sparsely forested strata rarely produced robust thresholds. This pattern was consistent in both the development area and the independent validation area.

These differences likely reflect two interacting factors. First, structural development of Scots pine is more predictable under well-drained and productive conditions, where long-term dominance leads to clearer crown expressions of ageing (Linder, 1998; Saarinen et al., 2022). Second, strata with few crowns or high structural variability provide weaker statistical support for identifying stable enrichment patterns, regardless of ecological relevance. Similar issues have been highlighted in previous ALS studies, where site heterogeneity reduces the interpretability of canopy metrics unless site conditions are explicitly controlled (Valbuena et al., 2014; Bonnet et al., 2015).

These results underline the importance of the stratification. By comparing trees only within similar site conditions, the analysis reduced the risk of confusing productivity-related differences with ageing signals. Without stratification, thresholds derived from productive sites would dominate the analysis and obstruct patterns elsewhere.

6.3 Accuracy and Limitations of the Classification

The field validation showed that the method is highly conservative. All trees classified as old-like displayed clear structural features associated with ageing, resulting in very high precision. This confirms that the selected threshold combinations correspond to meaningful structural patterns rather than random outliers.

However, recall was moderate, meaning that many structurally old trees were not detected. This outcome is expected for several reasons. Ageing in Scots pine is a gradual process, and many old individuals show only subtle or intermediate structural characteristics that may not exceed strict percentile thresholds (Linder, 1998; Huo et al., 2023). Additionally, the LIFT framework is designed to prioritize combinations of traits to co-occur more frequently than expected by chance. This inherently favours crowns with the strongest and most distinct structural expression of ageing, while excluding crowns that exhibit less pronounced ageing traits. As a result, the method emphasizes certainty over completeness, identifying a narrow subset of old-like trees with high confidence rather than attempting to capture the full population of structurally old individuals.

The field validation was also limited in size and focused on areas where old trees were already expected to occur. As a result, accuracy metrics should be interpreted with caution and viewed as indicative rather than definitive. Together, these factors support interpreting the method as a prioritization tool rather than a complete inventory method.

6.4 Methodological Strengths and Weaknesses

A key strength of the method is its reliance on national ALS datasets, which represent the baseline data available to forestry organizations and authorities in Sweden (Nilsson et al., 2016; Skogsstyrelsen, 2020). This makes the approach transferable and operationally realistic. The use of multi-temporal ALS to estimate height growth is another important strength, as growth suppression is a well-established indicator of structural ageing and cannot be derived from single-epoch data (Kozniewski et al., 2022).

The LIFT framework further strengthens the method. By focusing on combinations of traits that co-occur more often than expected by chance and not relying on fixed or arbitrary thresholds, local variations are accounted for. This aligns with the understanding that ageing is expressed through multivariate structural patterns rather than extreme values of single metrics (Huo et al., 2023).

A practical advantage of the method is that it can also be applied in areas where site conditions or stand age are already known. In such cases, site-based stratification is not as relevant, as trees are already being compared within a stratum that has known attributes. The LIFT-based approach can then be used to identify the trees that stand out most structurally relative to their

surroundings. For example, in a stand that is already known to be old, the method does not label all trees as old-like. Instead, it highlights those individuals with the strongest ageing-related crown characteristics. This makes the approach useful for not only locating old trees across heterogeneous landscapes, but also for identifying structurally exceptional trees where ecological value is expected to be high.

The main weakness lies in crown segmentation. Errors in separating adjacent crowns affected crown diameter and flatness, and the field observations showed that some predicted crowns represented multiple trees. This can inflate crown-level metrics and increase the likelihood that some crowns meet the threshold criteria, even though the signal represents multiple trees rather than an individual one. Such errors reduce the interpretability of crown geometry metrics and highlight segmentation quality as a critical limiting factor. Previous studies have noted that low point density in national ALS data contributes to these challenges, particularly in dense stands (Vauhkonen et al., 2014; Nilsson et al., 2016).

Additional limitations should also be acknowledged. The relatively low point density of national ALS data limits the ability to capture fine-scale crown features such as dead branches, cavities or hollows. As a result, the method identifies trees with old-like structural characteristics rather than confirming biological age. Structural maturity does not always correspond to chronological age, especially on sites where growth conditions strongly influence the crown form. Furthermore, some site-based strata contained relatively few crowns, which makes enrichment-based statistics more sensitive to random variation. Although this was partly addressed by applying the quality filters, it still means that structurally old trees occurring in rare or small strata may be overlooked.

Despite these limitations, the workflow is reproducible and practical. All processing steps were implemented through scripted workflows linked to a GIS environment, and all input data are either openly available or accessible through the Geodata Collaboration. The segmentation, stratification, LIFT analysis and classification steps are fully parameterized and documented, allowing the method to be rerun in new areas with only minor adjustments. This makes the approach reproducible by the same types of users who would realistically apply it in forestry or conservation planning.

6.5 Implications and Future Directions

Building on the identified strengths and limitations, it is interesting to discuss how the method can be further developed and how it can be applied in practice.

One clear area for improvement is crown segmentation. In dense forest stands, the low point density of national ALS data makes it difficult to separate overlapping pine crowns. A natural next step would therefore be to integrate high-resolution orthophotos or multispectral aerial imagery with ALS data. Previous studies have shown that combining height information with spectral data can improve crown segmentation, especially in complex canopies (Bonnet et al., 2015; Valbuena et al., 2014). Such an approach could improve segmentation accuracy and would also allow the method to be extended into other kinds of forests.

The individual tree analysis is a central strength of the proposed method. Rather than replacing this level of detail, future developments could focus on translating individual tree predictions into aggregated indicators. By summarizing the probabilities or counts of old-like trees, a kind of index could be created that reflects the presence and concentration of structurally old trees. Such an index would not diminish the individual tree analysis but serve as an additional support layer. This approach could bridge the eventual gap between fine-scale detection and forestry planning. Furthermore, weighing the index by e.g., site conditions could make it “safer”. As the results showed, the structurally old-like signal was the strongest on dry-fresh, mineral soils. This means that in more certain conditions, a higher level of certainty can be guaranteed.

Hyyppä et al. (2024) discusses the development of a national scale, individual tree-based forest information system derived from ALS data. While their system primarily focuses on production-related attributes, such as volume, biomass, or growth, the method in this thesis aligns well with the broader direction outlined by the authors. Instead of predicting timber-related variables, the method estimates the likelihood that individual trees exhibit old-like structural characteristics. Importantly, the approach presented here does not rely on specialized sensors, high density ALS or any other complex modelling frameworks. This makes it compatible with the scalable and operational GIS workflows discussed by Hyyppä et al. (2024).

7. Conclusion

This thesis demonstrates that national ALS data, despite its limitations, can meaningfully distinguish Scots pine individuals that exhibit old-like structural characteristics. The core finding is that structural ageing signals do not appear randomly across the landscape but form specific patterns depending on local variation. This confirms that individual tree ageing is detectable at a national data resolution when crown metrics are combined with site-aware stratification as well as an enrichment-based thresholding approach.

More importantly, the study shows that identifying structurally old trees does not require high-density LiDAR or local calibration. By relying solely on national datasets, the method demonstrates that existing data already contain enough information to guide conservation-decisions at tree level. This finding has practical implications: forestry planners can use routine national ALS products to prioritize retention trees and reduce field visits. The method therefore fills a gap between broad-scale forest inventories and fine-scale biodiversity needs.

The results also highlight that structural ageing is a rare but strongly patterned phenomenon. Old-like crowns consistently represent a very small fraction of all trees. However, their thresholds are strongest in sites containing dry-fresh mineral soils, indicating that these environments allow the pine to grow these structurally mature traits.

The study also clarifies the limits of what national ALS can achieve. Structural ageing can be detected, but fine-scale traits remain invisible. This invisibility puts a bigger emphasis on accurate crown segmentations, especially in dense stands. The method is therefore best understood as a prioritization tool: it identifies trees worth visiting in the field but will not provide a complete census of all old trees.

Finally, the findings point to several directions for future work. Larger field surveys are needed to quantify performance more robustly and to refine threshold selection. Incorporating multispectral data or more point dense ALS scans may improve sensitivity to additional ageing features. These developments would strengthen the method’s ability to support retention forestry.

In conclusion, the thesis shows that structurally old Scots pine can be detected at individual tree level using national ALS data. The presented method is not a complete solution, but it is a practical and scalable step toward improving the identification and retention of old trees.

References

Ågren, A. M., Hasselquist, E.M., Stendahl, J., Nilsson, M. B., & Paul, S. S. (2022). Delineating the distribution of mineral and peat soils at the landscape scale in northern boreal regions. *SOIL, 8*, 733–749. https://doi.org/10.5194/soil-8-733-2022

Ågren, A. M., Larson, J., Paul, S. S., Laudon, H., & Lidberg, W. (2021). Use of multiple LIDAR-derived digital terrain indices and machine learning for high-resolution national-scale soil moisture mapping of the Swedish forest landscape. *Geoderma*, *404*, 115280. https://doi.org/10.1016/j.geoderma.2021.115280

Bonnet, S., Gaulton, R., Lehaire, F., & Lejeune, P. (2015). Canopy Gap Mapping from Airborne Laser Scanning: An Assessment of the Positional and Geometrical Accuracy. *Remote Sensing, 7*(9), 11267–11294. https://doi.org/10.3390/rs70911267

Breidenbach, J., & Astrup, R. (2014). The Semi-Individual Tree Crown Approach. In Maltamo, M., Næsset, E., & Vauhkonen, J. (eds.) Forestry Applications of Airborne Laser Scanning. *Managing Forest Ecosystems*, vol 27. Springer, Dordrecht. https://doi.org/10.1007/978-94-017-8663-8_1

Fridman, J., Holm, S., Nilsson, M., Nilsson, P., Ringvall, A., & Ståhl, G. (2014). Adapting National Forest Inventories to changing requirements – the case of the Swedish National Forest Inventory at the turn of the 20th century. *Silva Fennica, 48*(3). https://doi.org/10.14214/sf.1095

Gavilan-Acuna, G., Coops, N.C., Tompalski, P., Roeser, D., & Varhola, A. (2025). The use and integration of airborne laser scanning and satellite time series data in precision forest management for plantations of fast-growing tree species. *Annals of Forest Science 82, 22*. https://doi.org/10.1186/s13595-025-01292-9

Han, J., Kamber, M., & Pei, J. (2012). *Data Mining: Concepts and Techniques*. 3rd ed. Elsevier.

Helms, A. J. (2004). Old-Growth: What Is It? *Journal of Forestry*, 102(3). 8–12. https://doi.org/10.1093/jof/102.3.8

Hijmans, R. J. (2023). *terra: Spatial Data Analysis* (R package version 1.8-80). https://cran.r-project.org/package=terra

Hirschmugl, M., Sobe, C., Di Filippo, A., Bär, H., Pichler, V., & Waser, L. T. (2023). Review on the possibilities of mapping old-growth temperate forests by remote sensing in Europe. *Environmental Modeling & Assessment*, 28, 764–785. https://doi.org/10.1007/s10666-023-09897-y

Holmgren, J., & Persson, Å. (2003). Identifying species of individual trees using airborne laser scanner. *Remote Sensing of Environment*, 90(4), 415–423. https://doi.org/10.1016/S0034-4257(03)00140-8

Huo, L., Strengbom, J., Lundmark, T., Westerfelt, P., & Lindberg, E. (2023). Estimating the conservation value of boreal forests using airborne laser scanning. *Ecological Indicators*, 147, 109946. https://doi.org/10.1016/j.ecolind.2023.109946

Hyyppä, M., Turppa, T., Hyyti, H., Yu, X., Handolin, H., Kukko, A., Hyyppä, J., & Virtanen, J-P. Concepts Towards Nation-Wide Individual Tree Data and Virtual Forests. *ISPRS International Journal of Geo-Information*, *13*(12), 424. https://doi.org/10.3390/ijgi13120424

Kozniewski, M., Kolendo, Ł., Ksepko, M., & Chmur, S. (2022). Tracking Individual Scots Pine (*Pinus sylvestris* L.) Height Growth Using Multi-Temporal ALS Data from North-Eastern Poland. *Remote Sensing*, *14*(17), 4170. https://doi.org/10.3390/rs14174170

Länsstyrelsen Uppsala. (n.d.-a). *Kungshamn-Morga*. [Retrieved 2025-11-25] https://www.lansstyrelsen.se/uppsala/besoksmal/naturreservat/kungshamn-morga.html?sv.target=12.382c024b1800285d5863a8a3&sv.12.382c024b1800285d5863a8a3.route=/&searchString=&counties=&municipalities=&reserveTypes=&natureTypes=&accessibility=&facilities=&sort=none

Länsstyrelsen Uppsala. (n.d.-b). *Norra Lunsen*. [Retrieved 2025-11-25]. https://www.lansstyrelsen.se/uppsala/besoksmal/naturreservat/norra-lunsen.html?sv.target=12.382c024b1800285d5863a8a3&sv.12.382c024b1800285d5863a8a3.route=/&searchString=&counties=&municipalities=&reserveTypes=&natureTypes=&accessibility=&facilities=&sort=none

Länsstyrelsen Uppsala. (n.d.-c). *Södra Lunsen*. [Retrieved 2025-11-25]. https://www.lansstyrelsen.se/uppsala/besoksmal/naturreservat/sodra-lunsen.html?sv.target=12.382c024b1800285d5863a8a3&sv.12.382c024b1800285d5863a8a3.route=/&searchString=&counties=&municipalities=&reserveTypes=&natureTypes=&accessibility=&facilities=&sort=none

Lantmäteriet. (2019). *GSD-Höjddata, grid 2+ [Digital elevation model, 2 x 2 m resolution]*. © Lantmäteriet. Gävle: Lantmäteriet.

Lantmäteriet. (2024a). *Product Description – Laser data Download, forest*. https://www.lantmateriet.se/globalassets/geodata/geodataprodukter/hojddata/e_pb_laserdata_nedladdning_skog.pdf

Lantmäteriet. (2024b). *Ortofoto RGBI 0.16 m latest, Ortophoto*. © Lantmäteriet. Gävle: Lantmäteriet.

Linder, P. (1998) Structural changes in two virgin boreal forest stands in central Sweden over 72 years. *Scandinavian Journal of Forest Research*, *13*(1-4), 451-461. https://doi.org/10.1080/02827589809383006

Manly, B., McDonald, L., Thomas, D., McDonald, T. L., & Erickson, W. P. (2002). *Resource selection by animals: Statistical Design and Analysis for Field Studies*. Springer Science & Business Media

Manning, C. D., Raghavan, P., & Schütze, H. (2009). *Introduction to information retrieval*. Cambridge University Press.

Næsset, E. (2002). Predicting forest stand and characteristics with airborne laser scanning using a practical two-stage procedure and field data. *Remote Sensing of Environment, 80*(1), 89–99. https://doi.org/10.1016/S0034-4257(01)00290-5

Naturvårdsverket. (2025). *Skyddade områden: naturreservet [Protected areas: nature reserves]*. INSPIRE Geoportal. https://inspire-geoportal.ec.europa.eu/srv/api/records/2921b01a-0baf-4702-a89f-9c5626c97844 [Retrieved 2025-11-13].

Nilsson, M., Nordkvist, K., Jonzén, J., Lindgren, N., Axensten, P., Wallerman, J., Egberth, M., Larsson, S., Nilsson, L., Eriksson, J., & Olsson, H. (2016). A nationwide forest attribute map of Sweden predicted using airborne laser scanning data and field data from the National Forest Inventory. *Remote Sensing of Environment, 194,* 447–454. https://doi.org/10.1016/j.rse.2016.10.022

Plowright, A. (2023). *ForestTools: Tools for Analyzing Remote Sensing Forest Data* (R package version 1.0.2). https://cran.r-project.org/package=ForestTools

Saarinen, N., Kankare, V., Huuskonen, S., Hynynen, J., Bianchi, S., Yrttimaa, T., Luoma, V., Junttila, S., Holopainen, M., Hyyppä, J., & Vastaranta, M. (2022). Effects of Stem Density on Crown Architecture of Scots Pine Trees. *Frontiers in plant science*, *13*, 817792. https://doi.org/10.3389/fpls.2022.817792

Schumacher, J., Hauglin, M., Astrup, R., & Breidenbach, J. (2020). Mapping forest age using National Forest Inventory, airborne laser scanning and Sentinel-2 data in Norway. *Forest Ecosystems*, 7, 60. https://doi.org/10.1186/s40663-020-00274-9

Siitonen, J. (2001). Forest Management, Coarse Woody Debris and Saproxylic Organisms: Fennoscandian Boreal Forests as an Example. *Ecological Bulletins*, *49*, 11-41. http://www.jstor.org/stable/20113262

SimWest2001. (2025). *old-pine-detection-ALS*. GitHub. https://github.com/SimWest2001/old-pine-detection-ALS

Skogforsk. (2024). Access to historical canopy height models for Idre–Särna and Lunsen–Kungshamn–Morgastudy areas (personal communication).

Skogsstyrelsen (2020). *Forest management in Sweden – Current practice and historical background*. Jönköping: Skogsstyrelsen. 2020:4.

Skogsstyrelsen (2024). *Skogliga Grunddata – Metadata Service (ArcGIS REST API)*. Available from: https://geodpags.skogsstyrelsen.se/arcgis/rest/services/Geodataportal/GeodataportalVisaSkogligaGrunddataMetadata/MapServer/0/query

Skogsstyrelsen (2025). *Skogliga grunddata – produktbeskrivning*. https://www.skogsstyrelsen.se/globalassets/sjalvservice/karttjanster/geodatatjanster/produktbeskrivningar/raster-skogliga-grunddata---produktbeskrivning.pdf [Retrieved 2025-12-08]

Skogsstyrelsen (n.d.). *Levande träd och buskar med naturvärden*. Jönköping: Skogsstyrelsen. https://www.skogsstyrelsen.se/globalassets/mer-om-skog/malbilder-for-god-miljohansyn/malbilder-trad-och-buskar-med-naturvarden-samt-dod-ved/levande-buskar-och-trad-med-naturvarden--exempel-2020.pdf [Retrieved 2025-11-11]

SLU (2025). *Produktbeskrivning: SLU skogsålder 2025*. *https://gis.slu.se/data/skogsdatalabbet/SLU_skogsalder_2025/dokument/SLU_skogsalder_2025_produktbeskrivning.docx*

Uppsala University (n.d.). UPPSALA, climate data for YEAR (Table 13). http://celsius.met.uu.se/climate_tables/?id=13 [Retrieved 2025-11-11]

Valbuena, R. (2014). Integrating Airborne Laser Scanning with Data from Global Navigation Satellite Systems and Optical Sensors. In Maltamo, M., Næsset, E., & Vauhkonen, J. (eds.) Forestry Applications of Airborne Laser Scanning. *Managing Forest Ecosystems*, vol 27. Springer, Dordrecht. https://doi.org/10.1007/978-94-017-8663-8_1

Vauhkonen, J., Maltamo, M., McRoberts, R. E., & Næsset, E. (2014). Introduction to Forestry Applications of Airborne Laser Scanning. In Maltamo, M., Næsset, E., & Vauhkonen, J. (eds.) Forestry Applications of Airborne Laser Scanning. *Managing Forest Ecosystems*, vol 27. Springer, Dordrecht. https://doi.org/10.1007/978-94-017-8663-8_1

Appendices

Appendix A.1 Strata Overview: Idre–Särna

Stratum ID	Elevation Band	Soil Moisture	Peat Depth	n (cells)	Hectares
1	L	Dry-fresh	Mineral soil	3 228 181	1291.27
2	L	Dry-fresh	≥ 30 cm	419	0.17
3	L	Dry-fresh	≥ 40 cm	57	0.02
4	L	Dry-fresh	≥ 50 cm	4	0.00
5	L	Fresh-moist	Mineral soil	404 388	161.76
6	L	Fresh-moist	≥ 30 cm	156 679	62.67
7	L	Fresh-moist	≥ 40 cm	96 254	38.50
8	L	Fresh-moist	≥ 50 cm	352 433	140.97
9	L	Moist-wet	Mineral soil	2 025	0.81
10	L	Moist-wet	≥ 30 cm	2 401	0.96
11	L	Moist-wet	≥ 40 cm	2 876	1.15
12	L	Moist-wet	≥ 50 cm	476 621	190.65
13	L	Water	Water	722 570	289.03
14	M	Dry-fresh	Mineral soil	2547010	1018.80
15	M	Dry-fresh	≥ 30 cm	316	0.13
16	M	Dry-fresh	≥ 40 cm	27	0.01
17	M	Dry-fresh	≥ 50 cm	3	0.00
18	M	Fresh-moist	Mineral soil	517 195	206.88
19	M	Fresh-moist	≥ 30 cm	231 464	92.59
20	M	Fresh-moist	≥ 40 cm	146 073	58.43
21	M	Fresh-moist	≥ 50 cm	580 931	232.37
22	M	Moist-wet	Mineral soil	1 355	0.54
23	M	Moist-wet	≥ 30 cm	1 659	0.66
24	M	Moist-wet	≥ 40 cm	2 449	0.98
25	M	Moist-wet	≥ 50 cm	881 336	352.53
26	M	Water	Water	87 841	35.14
27	H	Dry-fresh	Mineral soil	419 085	167.63
28	H	Dry-fresh	≥ 30 cm	26	0.01
29	H	Dry-fresh	≥ 40 cm	5	0.00
30	H	Dry-fresh	≥ 50 cm	0	0.00
31	H	Fresh-moist	Mineral soil	225 512	90.20
32	H	Fresh-moist	≥ 30 cm	113 771	45.51
33	H	Fresh-moist	≥ 40 cm	74 086	29.63
34	H	Fresh-moist	≥ 50 cm	175 540	70.22
35	H	Moist-wet	Mineral soil	18	0.01
36	H	Moist-wet	≥ 30 cm	115	0.05
37	H	Moist-wet	≥ 40 cm	369	0.15
38	H	Moist-wet	≥ 50 cm	174 644	69.86
39	H	Water	Water	4 019	1.61
40	Undef.	Undef.	Undef.	Undef.	Undef.
			Sum:	11 629 757	4651.9

A.2 Height Related Metrics

P95 Height (H)

					Metres				
Stratum ID	**Elevation Band**	**Soil Moisture**	**Peat Depth**	**n (crowns)**	**Min**	**Max**	**Mean**	**Median**	**Standard Deviation**
1	L	Dry-fresh	Mineral soil	243270	3.40	30.60	13.21	13.40	3.94
2	L	Dry-fresh	≥ 30 cm	34	5.80	20.90	13.54	13.35	4.16
3	L	Dry-fresh	≥ 40 cm	3	13.30	21.10	16.17	14.10	4.29
4	L	Dry-fresh	≥ 50 cm	0	-	-	-	-	-
5	L	Fresh-moist	Mineral soil	27044	3.50	29.00	13.00	13.00	4.06
6	L	Fresh-moist	≥ 30 cm	10666	4.00	29.10	12.70	12.50	4.10
7	L	Fresh-moist	≥ 40 cm	6504	4.00	28.80	12.47	12.20	4.15
8	L	Fresh-moist	≥ 50 cm	20695	3.60	28.10	11.12	10.70	3.79
9	L	Moist-wet	Mineral soil	104	4.90	21.40	13.79	14.10	3.03
10	L	Moist-wet	≥ 30 cm	118	4.60	27.70	13.24	13.50	3.77
11	L	Moist-wet	≥ 40 cm	125	5.90	25.80	12.67	12.60	3.98
12	L	Moist-wet	≥ 50 cm	12042	3.50	23.40	9.31	8.80	2.89
13	L	Water	Water	232	4.10	23.00	12.32	13.00	4.12
14	M	Dry-fresh	Mineral soil	199272	3.40	28.40	11.28	11.10	3.95
15	M	Dry-fresh	≥ 30 cm	18	5.70	18.10	12.62	14.35	4.35
16	M	Dry-fresh	≥ 40 cm	0	-	-	-	-	-
17	M	Dry-fresh	≥ 50 cm	1	7.60	7.60	7.60	7.60	0.00
18	M	Fresh-moist	Mineral soil	36022	3.50	28.00	10.89	10.40	3.71
19	M	Fresh-moist	≥ 30 cm	15894	3.90	27.50	10.89	10.40	3.66
20	M	Fresh-moist	≥ 40 cm	10133	3.60	26.40	11.10	10.70	3.74
21	M	Fresh-moist	≥ 50 cm	34652	3.60	27.30	10.47	10.00	3.51
22	M	Moist-wet	Mineral soil	59	5.10	23.30	12.29	12.80	4.03
23	M	Moist-wet	≥ 30 cm	90	5.80	22.20	11.74	11.65	3.44
24	M	Moist-wet	≥ 40 cm	129	4.40	22.10	9.90	9.30	3.52
25	M	Moist-wet	≥ 50 cm	25947	3.60	25.70	8.67	8.20	2.64
26	M	Water	Water	95	3.80	17.10	9.52	8.90	2.97
27	H	Dry-fresh	Mineral soil	34363	3.40	27.10	10.07	10.00	4.02
28	H	Dry-fresh	≥ 30 cm	0	-	-	-	-	-
29	H	Dry-fresh	≥ 40 cm	0	-	-	-	-	-
30	H	Dry-fresh	≥ 50 cm	0	-	-	-	-	-
31	H	Fresh-moist	Mineral soil	17724	3.60	30.30	11.16	11.40	3.72
32	H	Fresh-moist	≥ 30 cm	8714	3.70	27.80	11.63	11.70	3.72
33	H	Fresh-moist	≥ 40 cm	5594	3.70	29.40	12.03	11.90	3.78
34	H	Fresh-moist	≥ 50 cm	11929	3.60	29.60	12.07	11.70	3.96
35	H	Moist-wet	Mineral soil	1	16.80	16.80	16.80	16.80	0.00
36	H	Moist-wet	≥ 30 cm	12	6.70	23.70	14.32	14.90	5.15
37	H	Moist-wet	≥ 40 cm	23	5.20	22.30	12.58	11.20	4.82
38	H	Moist-wet	≥ 50 cm	5178	3.80	23.90	8.82	8.40	2.81
39	H	Water	Water	2	4.40	9.80	7.10	7.10	3.82
40	Undef.	Undef.	Undef.	74	5.90	20.40	13.50	13.50	3.01

A.3 Growth Related Metrics

Growth per year (G)

					Metres per Year				
Stratum ID	**Elevation Band**	**Soil Moisture**	**Peat Depth**	**n (crowns)**	**Min**	**Max**	**Mean**	**Median**	**Standard Deviation**
1	L	Dry-fresh	Mineral soil	243270	-1.98	2.09	0.26	0.25	0.18
2	L	Dry-fresh	≥ 30 cm	34	-0.01	0.56	0.23	0.22	0.15
3	L	Dry-fresh	≥ 40 cm	3	0.05	0.18	0.10	0.08	0.07
4	L	Dry-fresh	≥ 50 cm	0	-	-	-	-	-
5	L	Fresh-moist	Mineral soil	27044	-1.65	1.09	0.24	0.21	0.19
6	L	Fresh-moist	≥ 30 cm	10666	-1.76	1.45	0.22	0.20	0.19
7	L	Fresh-moist	≥ 40 cm	6504	-1.19	1.13	0.21	0.18	0.19
8	L	Fresh-moist	≥ 50 cm	20695	-1.39	1.45	0.15	0.11	0.17
9	L	Moist-wet	Mineral soil	104	-0.11	0.50	0.18	0.16	0.13
10	L	Moist-wet	≥ 30 cm	118	-0.11	0.71	0.20	0.19	0.15
11	L	Moist-wet	≥ 40 cm	125	-0.88	0.76	0.21	0.19	0.21
12	L	Moist-wet	≥ 50 cm	12042	-1.83	1.46	0.09	0.06	0.14
13	L	Water	Water	232	-0.33	1.70	0.13	0.09	0.20
14	M	Dry-fresh	Mineral soil	199272	-4.71	2.23	0.25	0.26	0.16
15	M	Dry-fresh	≥ 30 cm	18	-0.08	0.36	0.12	0.06	0.14
16	M	Dry-fresh	≥ 40 cm	0	-	-	-	-	-
17	M	Dry-fresh	≥ 50 cm	1	0.56	0.56	0.56	0.56	0.00
18	M	Fresh-moist	Mineral soil	36022	-1.70	1.53	0.21	0.21	0.17
19	M	Fresh-moist	≥ 30 cm	15894	-3.64	1.65	0.19	0.18	0.17
20	M	Fresh-moist	≥ 40 cm	10133	-0.88	1.29	0.17	0.15	0.17
21	M	Fresh-moist	≥ 50 cm	34652	-1.43	1.68	0.11	0.06	0.15
22	M	Moist-wet	Mineral soil	59	-0.10	0.39	0.10	0.08	0.10
23	M	Moist-wet	≥ 30 cm	90	-0.15	0.59	0.15	0.13	0.15
24	M	Moist-wet	≥ 40 cm	129	-0.16	0.86	0.23	0.19	0.21
25	M	Moist-wet	≥ 50 cm	25947	-4.99	1.65	0.05	0.03	0.11
26	M	Water	Water	95	-0.16	0.94	0.07	0.05	0.13
27	H	Dry-fresh	Mineral soil	34363	-4.83	1.03	0.28	0.31	0.17
28	H	Dry-fresh	≥ 30 cm	0	-	-	-	-	-
29	H	Dry-fresh	≥ 40 cm	0	-	-	-	-	-
30	H	Dry-fresh	≥ 50 cm	0	-	-	-	-	-
31	H	Fresh-moist	Mineral soil	17724	-3.61	0.98	0.25	0.29	0.19
32	H	Fresh-moist	≥ 30 cm	8714	-1.43	1.13	0.23	0.24	0.18
33	H	Fresh-moist	≥ 40 cm	5594	-2.01	1.06	0.20	0.18	0.18
34	H	Fresh-moist	≥ 50 cm	11929	-1.65	1.05	0.13	0.09	0.17
35	H	Moist-wet	Mineral soil	1	0.01	0.01	0.01	0.01	0.00
36	H	Moist-wet	≥ 30 cm	12	0.01	0.23	0.11	0.08	0.07
37	H	Moist-wet	≥ 40 cm	23	-0.20	0.23	0.08	0.08	0.10
38	H	Moist-wet	≥ 50 cm	5178	-1.28	0.60	0.04	0.03	0.09
39	H	Water	Water	2	-0.11	0.06	-0.03	-0.03	0.12
40	Undef.	Undef.	Undef.	74	-0.16	1.56	0.20	0.14	0.24

A.4 Crown Diameter Metrics

Crown diameter (C)

					Metres				
Stratum ID	**Elevation Band**	**Soil Moisture**	**Peat Depth**	**n (crowns)**	**Min**	**Max**	**Mean**	**Median**	**Standard Deviation**
1	L	Dry-fresh	Mineral soil	243270	2.76	17.04	6.43	6.38	1.46
2	L	Dry-fresh	≥ 30 cm	34	3.57	9.24	6.63	6.86	1.68
3	L	Dry-fresh	≥ 40 cm	3	6.08	7.98	7.00	6.96	0.95
4	L	Dry-fresh	≥ 50 cm	0	-	-	-	-	-
5	L	Fresh-moist	Mineral soil	27044	2.76	15.68	6.54	6.48	1.57
6	L	Fresh-moist	≥ 30 cm	10666	2.76	14.58	6.54	6.48	1.61
7	L	Fresh-moist	≥ 40 cm	6504	2.76	15.59	6.55	6.48	1.64
8	L	Fresh-moist	≥ 50 cm	20695	2.76	14.76	6.20	6.18	1.70
9	L	Moist-wet	Mineral soil	104	2.99	12.72	6.58	6.48	1.61
10	L	Moist-wet	≥ 30 cm	118	2.76	11.56	6.44	6.53	1.51
11	L	Moist-wet	≥ 40 cm	125	3.39	13.26	6.61	6.58	1.81
12	L	Moist-wet	≥ 50 cm	12042	2.76	15.35	5.51	5.41	1.70
13	L	Water	Water	232	2.76	11.51	7.49	7.74	2.02
14	M	Dry-fresh	Mineral soil	199272	2.76	16.35	6.07	6.08	1.58
15	M	Dry-fresh	≥ 30 cm	18	2.76	8.67	6.64	7.22	1.88
16	M	Dry-fresh	≥ 40 cm	0	-	-	-	-	-
17	M	Dry-fresh	≥ 50 cm	1	2.76	2.76	2.76	2.76	0.00
18	M	Fresh-moist	Mineral soil	36022	2.76	14.88	6.10	6.08	1.64
19	M	Fresh-moist	≥ 30 cm	15894	2.76	15.84	6.12	6.08	1.65
20	M	Fresh-moist	≥ 40 cm	10133	2.76	14.09	6.21	6.18	1.67
21	M	Fresh-moist	≥ 50 cm	34652	2.76	17.15	6.01	5.97	1.70
22	M	Moist-wet	Mineral soil	59	2.76	11.78	6.92	6.96	2.06
23	M	Moist-wet	≥ 30 cm	90	2.76	11.11	6.47	6.53	1.78
24	M	Moist-wet	≥ 40 cm	129	2.76	9.90	5.75	5.75	1.56
25	M	Moist-wet	≥ 50 cm	25947	2.76	13.30	5.23	5.05	1.64
26	M	Water	Water	95	2.76	11.73	6.30	6.28	1.82
27	H	Dry-fresh	Mineral soil	34363	2.76	13.54	5.84	5.75	1.60
28	H	Dry-fresh	≥ 30 cm	0	-	-	-	-	-
29	H	Dry-fresh	≥ 40 cm	0	-	-	-	-	-
30	H	Dry-fresh	≥ 50 cm	0	-	-	-	-	-
31	H	Fresh-moist	Mineral soil	17724	2.76	12.91	6.11	6.08	1.53
32	H	Fresh-moist	≥ 30 cm	8714	2.76	14.05	6.22	6.18	1.54
33	H	Fresh-moist	≥ 40 cm	5594	2.76	12.96	6.37	6.28	1.51
34	H	Fresh-moist	≥ 50 cm	11929	2.76	16.31	6.40	6.38	1.63
35	H	Moist-wet	Mineral soil	1	6.08	6.08	6.08	6.08	0.00
36	H	Moist-wet	≥ 30 cm	12	3.39	8.52	5.94	6.08	1.50
37	H	Moist-wet	≥ 40 cm	23	2.99	10.34	6.53	6.28	1.84
38	H	Moist-wet	≥ 50 cm	5178	2.76	13.26	5.22	5.05	1.67
39	H	Water	Water	2	3.19	7.57	5.38	5.38	3.10
40	Undef.	Undef.	Undef.	74	2.76	13.54	6.73	6.68	2.35

A.5 Crown Flatness Metrics

Crown flatness (F)

					Metres				
Stratum ID	**Elevation Band**	**Soil Moisture**	**Peat Depth**	**n (crowns)**	**Min**	**Max**	**Mean**	**Median**	**Standard Deviation**
1	L	Dry-fresh	Mineral soil	243270	0.00	14.24	4.42	4.36	1.79
2	L	Dry-fresh	≥ 30 cm	34	1.24	9.90	4.63	4.79	1.95
3	L	Dry-fresh	≥ 40 cm	3	3.98	8.97	5.99	5.03	2.63
4	L	Dry-fresh	≥ 50 cm	0	-	-	-	-	-
5	L	Fresh-moist	Mineral soil	27044	0.00	13.96	4.44	4.34	1.92
6	L	Fresh-moist	≥ 30 cm	10666	0.05	14.50	4.35	4.20	1.98
7	L	Fresh-moist	≥ 40 cm	6504	0.00	13.46	4.26	4.08	1.98
8	L	Fresh-moist	≥ 50 cm	20695	0.03	13.36	3.71	3.49	1.92
9	L	Moist-wet	Mineral soil	104	0.60	9.05	4.94	5.08	1.76
10	L	Moist-wet	≥ 30 cm	118	0.47	9.89	4.60	4.62	1.81
11	L	Moist-wet	≥ 40 cm	125	0.44	10.89	4.55	4.25	2.04
12	L	Moist-wet	≥ 50 cm	12042	0.01	12.79	2.91	2.71	1.67
13	L	Water	Water	232	0.00	9.36	4.02	4.31	2.42
14	M	Dry-fresh	Mineral soil	199272	0.00	15.71	3.73	3.57	1.81
15	M	Dry-fresh	≥ 30 cm	18	1.22	6.78	4.11	4.24	1.83
16	M	Dry-fresh	≥ 40 cm	0	-	-	-	-	-
17	M	Dry-fresh	≥ 50 cm	1	2.20	2.20	2.20	2.20	0.00
18	M	Fresh-moist	Mineral soil	36022	0.00	13.59	3.66	3.45	1.78
19	M	Fresh-moist	≥ 30 cm	15894	0.04	12.95	3.66	3.46	1.79
20	M	Fresh-moist	≥ 40 cm	10133	0.06	13.83	3.72	3.54	1.80
21	M	Fresh-moist	≥ 50 cm	34652	0.00	14.63	3.40	3.21	1.81
22	M	Moist-wet	Mineral soil	59	0.55	9.03	4.40	4.39	1.98
23	M	Moist-wet	≥ 30 cm	90	0.71	8.55	4.16	4.00	1.80
24	M	Moist-wet	≥ 40 cm	129	0.21	8.26	3.34	3.03	1.74
25	M	Moist-wet	≥ 50 cm	25947	0.00	12.82	2.47	2.24	1.55
26	M	Water	Water	95	0.14	7.49	3.17	3.00	1.63
27	H	Dry-fresh	Mineral soil	34363	0.06	13.52	3.18	2.91	1.72
28	H	Dry-fresh	≥ 30 cm	0	-	-	-	-	-
29	H	Dry-fresh	≥ 40 cm	0	-	-	-	-	-
30	H	Dry-fresh	≥ 50 cm	0	-	-	-	-	-
31	H	Fresh-moist	Mineral soil	17724	0.04	11.87	3.52	3.40	1.63
32	H	Fresh-moist	≥ 30 cm	8714	0.13	12.63	3.64	3.52	1.64
33	H	Fresh-moist	≥ 40 cm	5594	0.20	14.13	3.78	3.64	1.68
34	H	Fresh-moist	≥ 50 cm	11929	0.03	15.75	3.86	3.67	1.85
35	H	Moist-wet	Mineral soil	1	6.95	6.95	6.95	6.95	0.00
36	H	Moist-wet	≥ 30 cm	12	1.01	6.87	3.66	3.79	1.86
37	H	Moist-wet	≥ 40 cm	23	0.91	6.46	3.63	3.57	1.77
38	H	Moist-wet	≥ 50 cm	5178	0.02	12.75	2.52	2.28	1.65
39	H	Water	Water	2	0.03	2.39	1.21	1.21	1.67
40	Undef.	Undef.	Undef.	74	1.23	11.38	5.08	4.71	2.37

Appendix B.1 Strata Overview: Lunsen–Kungshamn–Morga

Stratum ID	Elevation Band	Soil Moisture	Peat Depth	n (cells)	Hectares
1	L	Dry-fresh	Mineral soil	575 597	230.24
2	L	Dry-fresh	≥ 30 cm	310	0.12
3	L	Dry-fresh	≥ 40 cm	25	0.01
4	L	Dry-fresh	≥ 50 cm	1	0.00
5	L	Fresh-moist	Mineral soil	34 164	13.67
6	L	Fresh-moist	≥ 30 cm	3 241	1.30
7	L	Fresh-moist	≥ 40 cm	1 247	0.50
8	L	Fresh-moist	≥ 50 cm	895	0.36
9	L	Moist-wet	Mineral soil	327	0.13
10	L	Moist-wet	≥ 30 cm	574	0.23
11	L	Moist-wet	≥ 40 cm	412	0.16
12	L	Moist-wet	≥ 50 cm	2 855	1.14
13	L	Water	Water	671 264	268.51
14	M	Dry-fresh	Mineral soil	1 689 735	675.89
15	M	Dry-fresh	≥ 30 cm	776	0.31
16	M	Dry-fresh	≥ 40 cm	65	0.03
17	M	Dry-fresh	≥ 50 cm	8	0.00
18	M	Fresh-moist	Mineral soil	234 380	93.75
19	M	Fresh-moist	≥ 30 cm	23 777	9.51
20	M	Fresh-moist	≥ 40 cm	9 088	3.64
21	M	Fresh-moist	≥ 50 cm	34 014	13.61
22	M	Moist-wet	Mineral soil	56	0.02
23	M	Moist-wet	≥ 30 cm	361	0.14
24	M	Moist-wet	≥ 40 cm	623	0.25
25	M	Moist-wet	≥ 50 cm	10 482	4.19
26	M	Water	Water	401	0.16
					0.00
27	H	Dry-fresh	Mineral soil	1 745 997	698.40
28	H	Dry-fresh	≥ 30 cm	151	0.06
29	H	Dry-fresh	≥ 40 cm	1	0.00
30	H	Dry-fresh	≥ 50 cm		0.00
31	H	Fresh-moist	Mineral soil	212 796	85.12
32	H	Fresh-moist	≥ 30 cm	51 423	20.57
33	H	Fresh-moist	≥ 40 cm	24 239	9.70
34	H	Fresh-moist	≥ 50 cm	92 840	37.14
35	H	Moist-wet	Mineral soil	202	0.08
36	H	Moist-wet	≥ 30 cm	486	0.19
37	H	Moist-wet	≥ 40 cm	276	0.11
38	H	Moist-wet	≥ 50 cm	81 130	32.45
39	H	Water	Water	5	0.00
40	Undef.	Undef.	Undef.	Undef.	Undef.
			Sum:	5 504 224	2201.69

B.2 Height Related Metrics

P95 Height (H)

					Metres				
Stratum ID	**Elevation Band**	**Soil Moisture**	**Peat Depth**	**n (crowns)**	**Min**	**Max**	**Mean**	**Median**	**Standard Deviation**
1	L	Dry-fresh	Mineral soil	21436	3.10	39.30	19.47	20.40	6.73
2	L	Dry-fresh	≥ 30 cm	5	10.00	18.00	14.06	14.40	3.65
3	L	Dry-fresh	≥ 40 cm	0	-	-	-	-	-
4	L	Dry-fresh	≥ 50 cm	0	-	-	-	-	-
5	L	Fresh-moist	Mineral soil	871	3.20	33.60	14.81	14.00	8.01
6	L	Fresh-moist	≥ 30 cm	120	3.30	31.10	15.00	15.60	6.90
7	L	Fresh-moist	≥ 40 cm	62	6.20	27.80	17.09	17.35	5.88
8	L	Fresh-moist	≥ 50 cm	43	4.20	26.90	17.18	17.30	4.95
9	L	Moist-wet	Mineral soil	6	8.50	18.70	14.23	14.30	3.98
10	L	Moist-wet	≥ 30 cm	2	8.70	21.90	15.30	15.30	9.33
11	L	Moist-wet	≥ 40 cm	5	5.10	27.30	17.04	21.60	9.78
12	L	Moist-wet	≥ 50 cm	33	4.50	25.10	10.45	7.20	6.29
13	L	Water	Water	469	3.30	27.10	12.81	12.90	4.96
14	M	Dry-fresh	Mineral soil	100 589	3.30	49.20	20.41	21.00	5.27
15	M	Dry-fresh	≥ 30 cm	5	4.10	22.70	14.76	20.30	9.73
16	M	Dry-fresh	≥ 40 cm	0	-	-	-	-	-
17	M	Dry-fresh	≥ 50 cm	0	-	-	-	-	-
18	M	Fresh-moist	Mineral soil	12 609	3.30	35.00	19.39	20.10	5.59
19	M	Fresh-moist	≥ 30 cm	1 329	3.60	31.40	18.92	19.50	5.09
20	M	Fresh-moist	≥ 40 cm	498	4.00	29.20	18.87	19.60	4.96
21	M	Fresh-moist	≥ 50 cm	2 246	3.90	29.80	19.24	19.90	4.89
22	M	Moist-wet	Mineral soil	2	9.00	9.00	9.00	9.00	0.00
23	M	Moist-wet	≥ 30 cm	3	12.50	13.40	12.90	12.80	0.46
24	M	Moist-wet	≥ 40 cm	11	6.10	16.20	12.67	13.50	2.86
25	M	Moist-wet	≥ 50 cm	776	4.20	28.70	17.32	17.40	4.87
26	M	Water	Water	10	4.10	14.70	7.85	5.85	4.04
27	H	Dry-fresh	Mineral soil	137538	3.40	41.20	16.55	16.50	4.10
28	H	Dry-fresh	≥ 30 cm	12	10.80	23.10	17.05	17.10	4.45
29	H	Dry-fresh	≥ 40 cm	0	-	-	-	-	-
30	H	Dry-fresh	≥ 50 cm	0	-	-	-	-	-
31	H	Fresh-moist	Mineral soil	17 419	3.40	31.10	16.66	17.00	4.58
32	H	Fresh-moist	≥ 30 cm	4 206	3.60	30.30	16.08	16.40	4.31
33	H	Fresh-moist	≥ 40 cm	1 887	3.80	30.20	15.21	15.40	4.40
34	H	Fresh-moist	≥ 50 cm	7 015	3.60	30.10	12.90	12.70	4.18
35	H	Moist-wet	Mineral soil	21	6.70	17.30	12.89	12.60	2.83
36	H	Moist-wet	≥ 30 cm	15	8.20	15.80	12.55	12.90	2.17
37	H	Moist-wet	≥ 40 cm	19	6.40	19.70	13.93	15.40	4.09
38	H	Moist-wet	≥ 50 cm	5 727	3.60	23.80	10.88	10.60	3.70
39	H	Water	Water	0	-	-	-	-	-
40	Undef.	Undef.	Undef.	4	5.70	9.40	6.88	6.20	1.71

B.3 Growth Related Metrics

Growth per year (G)

					Metres per Year				
Stratum ID	**Elevation Band**	**Soil Moisture**	**Peat Depth**	**n (crowns)**	**Min**	**Max**	**Mean**	**Median**	**Standard Deviation**
1	L	Dry-fresh	Mineral soil	21436	-2.86	2.54	0.11	0.10	0.30
2	L	Dry-fresh	≥ 30 cm	5	-0.11	1.03	0.46	0.44	0.52
3	L	Dry-fresh	≥ 40 cm	0	-	-	-	-	-
4	L	Dry-fresh	≥ 50 cm	0	-	-	-	-	-
5	L	Fresh-moist	Mineral soil	871	-2.28	1.13	0.18	0.10	0.39
6	L	Fresh-moist	≥ 30 cm	120	-0.58	1.08	0.23	0.11	0.33
7	L	Fresh-moist	≥ 40 cm	62	-0.43	1.15	0.22	0.18	0.31
8	L	Fresh-moist	≥ 50 cm	43	-0.33	0.93	0.24	0.21	0.25
9	L	Moist-wet	Mineral soil	6	-0.08	0.70	0.24	0.14	0.31
10	L	Moist-wet	≥ 30 cm	2	-0.26	1.09	0.41	0.41	0.95
11	L	Moist-wet	≥ 40 cm	5	-0.05	1.03	0.34	0.06	0.47
12	L	Moist-wet	≥ 50 cm	33	-0.70	1.18	0.24	0.20	0.45
13	L	Water	Water	469	-1.45	1.55	0.06	0.06	0.32
14	M	Dry-fresh	Mineral soil	100 589	-3.41	3.58	0.26	0.26	0.35
15	M	Dry-fresh	≥ 30 cm	5	-2.69	0.56	-0.22	0.26	1.39
16	M	Dry-fresh	≥ 40 cm	0	-	-	-	-	-
17	M	Dry-fresh	≥ 50 cm	0	-	-	-	-	-
18	M	Fresh-moist	Mineral soil	12 609	-3.48	3.26	0.25	0.26	0.47
19	M	Fresh-moist	≥ 30 cm	1 329	-2.78	3.05	0.25	0.26	0.39
20	M	Fresh-moist	≥ 40 cm	498	-2.38	3.11	0.25	0.24	0.34
21	M	Fresh-moist	≥ 50 cm	2 246	-2.56	2.74	0.21	0.21	0.29
22	M	Moist-wet	Mineral soil	2	-0.05	0.75	0.35	0.35	0.57
23	M	Moist-wet	≥ 30 cm	3	0.08	0.59	0.38	0.48	0.27
24	M	Moist-wet	≥ 40 cm	11	-0.50	0.54	0.08	0.09	0.29
25	M	Moist-wet	≥ 50 cm	776	-1.33	1.04	0.19	0.19	0.18
26	M	Water	Water	10	-0.09	0.65	0.15	0.09	0.23
27	H	Dry-fresh	Mineral soil	137538	-3.05	3.88	0.24	0.21	0.19
28	H	Dry-fresh	≥ 30 cm	12	-0.05	0.51	0.21	0.15	0.17
29	H	Dry-fresh	≥ 40 cm	0	-	-	-	-	-
30	H	Dry-fresh	≥ 50 cm	0	-	-	-	-	-
31	H	Fresh-moist	Mineral soil	17 419	-2.89	1.79	0.28	0.25	0.24
32	H	Fresh-moist	≥ 30 cm	4 206	-2.01	1.04	0.23	0.21	0.21
33	H	Fresh-moist	≥ 40 cm	1 887	-1.65	1.03	0.20	0.19	0.21
34	H	Fresh-moist	≥ 50 cm	7 015	-2.18	1.31	0.18	0.18	0.17
35	H	Moist-wet	Mineral soil	21	0.03	0.49	0.16	0.11	0.13
36	H	Moist-wet	≥ 30 cm	15	0.03	0.34	0.14	0.14	0.09
37	H	Moist-wet	≥ 40 cm	19	-0.53	0.63	0.14	0.15	0.21
38	H	Moist-wet	≥ 50 cm	5 727	-1.59	1.25	0.15	0.15	0.19
39	H	Water	Water	0	-	-	-	-	-
40	Undef.	Undef.	Undef.	4	-0.04	0.16	0.07	0.07	0.11

B.4 Crown Diameter Metrics

Crown diameter (C)

					Metres				
Stratum ID	**Elevation Band**	**Soil Moisture**	**Peat Depth**	**n (crowns)**	**Min**	**Max**	**Mean**	**Median**	**Standard Deviation**
1	L	Dry-fresh	Mineral soil	21436	2.76	19.74	8.00	7.82	2.39
2	L	Dry-fresh	≥ 30 cm	5	5.05	11.23	7.48	7.57	2.60
3	L	Dry-fresh	≥ 40 cm	0	-	-	-	-	-
4	L	Dry-fresh	≥ 50 cm	0	-	-	-	-	-
5	L	Fresh-moist	Mineral soil	871	2.76	16.96	7.37	6.96	2.72
6	L	Fresh-moist	≥ 30 cm	120	2.76	17.08	7.70	7.27	3.01
7	L	Fresh-moist	≥ 40 cm	62	2.99	13.54	7.93	7.57	2.66
8	L	Fresh-moist	≥ 50 cm	43	2.99	15.39	7.25	7.31	2.32
9	L	Moist-wet	Mineral soil	6	4.79	9.90	7.27	7.29	2.03
10	L	Moist-wet	≥ 30 cm	2	4.07	5.53	4.80	4.80	1.03
11	L	Moist-wet	≥ 40 cm	5	2.76	15.72	8.78	7.57	5.18
12	L	Moist-wet	≥ 50 cm	33	2.99	12.87	6.53	5.75	2.58
13	L	Water	Water	469	2.76	16.55	8.13	8.06	2.36
14	M	Dry-fresh	Mineral soil	100 589	2.76	24.17	7.44	7.31	1.79
15	M	Dry-fresh	≥ 30 cm	5	2.99	7.65	5.36	5.53	2.06
16	M	Dry-fresh	≥ 40 cm	0	-	-	-	-	-
17	M	Dry-fresh	≥ 50 cm	0	-	-	-	-	-
18	M	Fresh-moist	Mineral soil	12 609	2.76	21.97	7.11	7.05	1.77
19	M	Fresh-moist	≥ 30 cm	1 329	2.76	16.47	7.19	7.14	1.85
20	M	Fresh-moist	≥ 40 cm	498	2.76	13.49	7.32	7.31	1.65
21	M	Fresh-moist	≥ 50 cm	2 246	2.76	14.36	7.24	7.14	1.64
22	M	Moist-wet	Mineral soil	2	2.76	6.28	4.52	4.52	2.49
23	M	Moist-wet	≥ 30 cm	3	6.18	12.31	8.60	7.31	3.26
24	M	Moist-wet	≥ 40 cm	11	3.19	11.40	6.13	6.08	2.21
25	M	Moist-wet	≥ 50 cm	776	2.76	13.16	7.06	6.96	1.60
26	M	Water	Water	10	3.74	13.45	7.59	6.95	2.96
27	H	Dry-fresh	Mineral soil	137538	2.76	17.70	7.50	7.40	1.57
28	H	Dry-fresh	≥ 30 cm	12	3.57	11.34	7.73	7.86	2.40
29	H	Dry-fresh	≥ 40 cm	0	-	-	-	-	-
30	H	Dry-fresh	≥ 50 cm	0	-	-	-	-	-
31	H	Fresh-moist	Mineral soil	17 419	2.76	15.14	7.24	7.14	1.61
32	H	Fresh-moist	≥ 30 cm	4 206	2.76	15.05	7.31	7.23	1.70
33	H	Fresh-moist	≥ 40 cm	1 887	2.76	14.18	7.44	7.31	1.73
34	H	Fresh-moist	≥ 50 cm	7 015	2.76	19.02	7.35	7.23	1.76
35	H	Moist-wet	Mineral soil	21	6.58	12.26	9.22	9.71	1.72
36	H	Moist-wet	≥ 30 cm	15	4.92	12.05	8.70	8.59	1.94
37	H	Moist-wet	≥ 40 cm	19	4.51	14.36	8.75	8.81	2.67
38	H	Moist-wet	≥ 50 cm	5 727	2.76	14.32	6.63	6.58	1.83
39	H	Water	Water	0	-	-	-	-	-
40	Undef.	Undef.	Undef.	4	4.65	12.21	8.20	7.97	3.25

B.5 Crown Flatness Metrics

Crown flatness (F)

					Metres				
Stratum ID	**Elevation Band**	**Soil Moisture**	**Peat Depth**	**n (crowns)**	**Min**	**Max**	**Mean**	**Median**	**Standard Deviation**
1	L	Dry-fresh	Mineral soil	21436	0.00	26.06	5.91	5.77	2.89
2	L	Dry-fresh	≥ 30 cm	5	3.03	7.32	5.08	4.69	1.91
3	L	Dry-fresh	≥ 40 cm	0	-	-	-	-	-
4	L	Dry-fresh	≥ 50 cm	0	-	-	-	-	-
5	L	Fresh-moist	Mineral soil	871	0.06	18.40	4.84	4.27	3.46
6	L	Fresh-moist	≥ 30 cm	120	0.05	14.15	5.13	5.40	2.94
7	L	Fresh-moist	≥ 40 cm	62	1.39	16.43	6.64	6.59	3.12
8	L	Fresh-moist	≥ 50 cm	43	0.69	10.50	5.98	6.27	2.36
9	L	Moist-wet	Mineral soil	6	2.37	9.56	6.19	6.38	2.80
10	L	Moist-wet	≥ 30 cm	2	3.70	9.39	6.55	6.55	4.02
11	L	Moist-wet	≥ 40 cm	5	0.28	10.06	6.19	8.16	4.36
12	L	Moist-wet	≥ 50 cm	33	0.61	9.49	3.69	2.33	2.86
13	L	Water	Water	469	0.02	14.18	4.67	4.88	2.49
14	M	Dry-fresh	Mineral soil	100 589	0.00	33.04	5.64	5.34	2.66
15	M	Dry-fresh	≥ 30 cm	5	0.57	11.19	4.36	3.44	4.43
16	M	Dry-fresh	≥ 40 cm	0	-	-	-	-	-
17	M	Dry-fresh	≥ 50 cm	0	-	-	-	-	-
18	M	Fresh-moist	Mineral soil	12 609	0.05	19.79	5.65	5.28	2.94
19	M	Fresh-moist	≥ 30 cm	1 329	0.20	19.38	5.56	5.21	2.85
20	M	Fresh-moist	≥ 40 cm	498	0.31	16.71	5.15	4.67	2.70
21	M	Fresh-moist	≥ 50 cm	2 246	0.20	15.49	4.42	3.97	2.25
22	M	Moist-wet	Mineral soil	2	2.20	4.30	3.25	3.25	1.48
23	M	Moist-wet	≥ 30 cm	3	3.10	5.56	4.39	4.49	1.23
24	M	Moist-wet	≥ 40 cm	11	1.43	6.76	4.93	5.24	1.59
25	M	Moist-wet	≥ 50 cm	776	0.27	14.13	4.33	4.04	2.05
26	M	Water	Water	10	0.41	7.97	2.87	1.74	2.49
27	H	Dry-fresh	Mineral soil	137538	0.02	32.40	4.22	3.98	1.86
28	H	Dry-fresh	≥ 30 cm	12	1.01	6.14	3.43	3.08	1.63
29	H	Dry-fresh	≥ 40 cm	0	-	-	-	-	-
30	H	Dry-fresh	≥ 50 cm	0	-	-	-	-	-
31	H	Fresh-moist	Mineral soil	17 419	0.10	15.23	3.97	3.64	1.93
32	H	Fresh-moist	≥ 30 cm	4 206	0.16	13.79	3.74	3.43	1.83
33	H	Fresh-moist	≥ 40 cm	1 887	0.18	12.89	3.64	3.28	1.82
34	H	Fresh-moist	≥ 50 cm	7 015	0.14	13.40	3.17	2.87	1.60
35	H	Moist-wet	Mineral soil	21	1.55	8.51	3.94	3.89	1.46
36	H	Moist-wet	≥ 30 cm	15	1.47	4.43	3.13	2.95	0.79
37	H	Moist-wet	≥ 40 cm	19	1.75	8.47	4.04	3.23	1.86
38	H	Moist-wet	≥ 50 cm	5 727	0.08	13.81	2.84	2.47	1.73
39	H	Water	Water	0	-	-	-	-	-
40	Undef.	Undef.	Undef.	4	1.42	3.64	2.04	1.55	1.07

Appendix C

1. Tree type:

☐ Model-tree ☐ Proximal tree ☐ 30-metre tree

2. Diameter at breast height (DBH)

3. Does the trunk exhibit fire damage?

☐ Yes ☐ No

4. Are there any bracket fungus visible?

☐ Yes ☐ No

5. Are there any visible cavities?

☐ Yes ☐ No

6. Is the bark of a different structure? (rough, crocodile/armoured bark)

☐ Yes ☐ No

7. Does the tree have thick branches?

☐ Yes ☐ No

8. Does the tree have dead branches?

☐ Yes ☐ No

9. Is the crown shape flat?

☐ Yes ☐ No

10. Is the tree considered to have the character of an older tree?

☐ Yes ☐ No

Appendix D

D.1 Overall Workflow

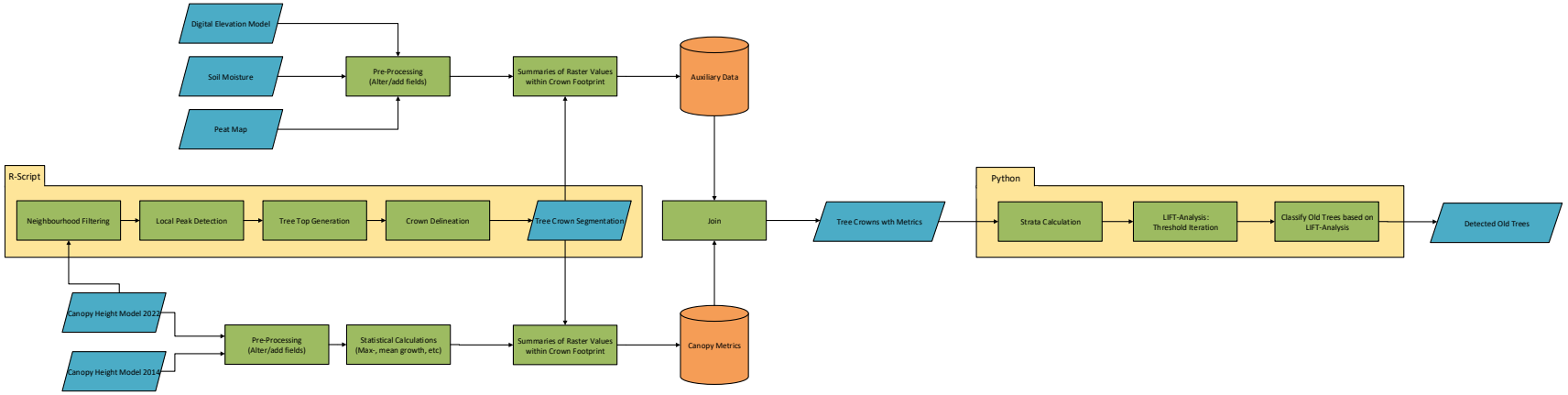

D.2 LIFT Workflow

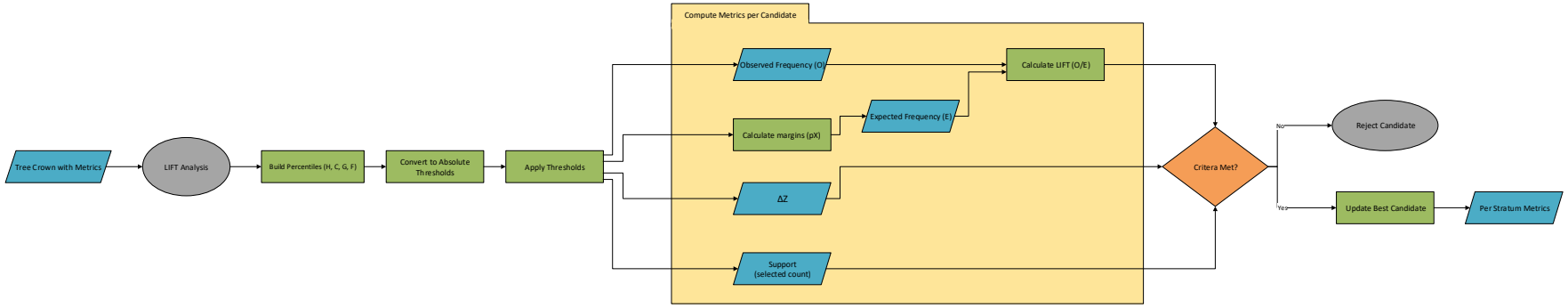

Appendix E

How Do We Compare One Tree to Every Other Tree?

LIFT tests different combinations of thresholds for the canopy metrics within each strata:

- Height
- Crown width
- Crown flatness
- Height growth

Example (purely theoretical, no tree grows 4 m/year):

- Height > 10 m, Width > 1 m, Flatness < 5 m, Growth < 4 m/year
- Height > 12 m, Width > 1.3 m, Flatness < 3.5 m, Growth < 2.8 m/year
- Height > 15 m, Width > 3.5 m, Flatness < 3 m, Growth < 2 m/year
- Height > 17 m, Width > 4.0 m, Flatness < 2.5 m, Growth < 1.5 m/year

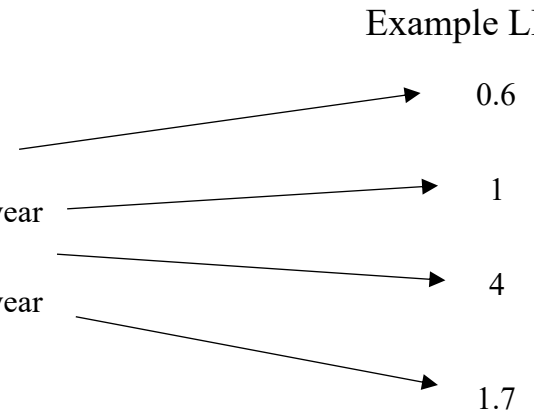

For every candidate, the quality filters remove candidates that does not fulfil all three filters, and the LIFT-value is calculated.

In this theoretical example, the model would save threshold 3, because that combination resulted in the highest LIFT-value.

The LIFT-value is calculated as $\frac{Observed\ Prevalence}{Expected\ Prevalence}$.

Expected Prevalence

Here is a theoretical example of how the expected prevalence is calculated.

How many percent of all trees are:

- Higher than 10 metres
- Wider than 4 metres
- Flatter than 3 metres
- Grows less than 1.3 metres / year

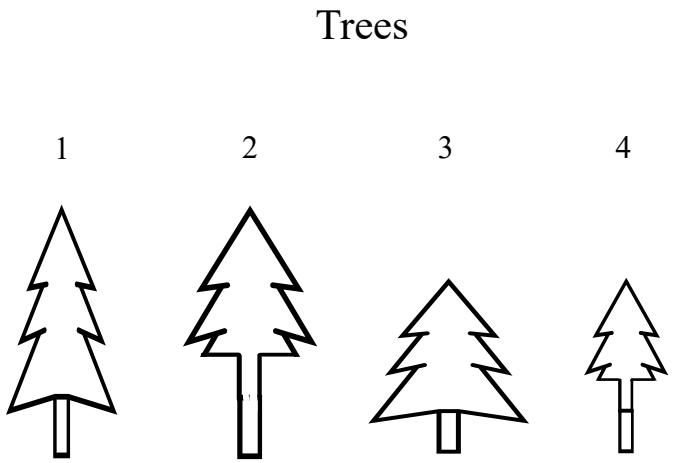

- Tree 1 and 2 > 10 metres ➔ 50% of all trees
- Tree 2 and 3 has a crown width > 4 metres ➔ 50% of all trees
- Tree 2 and 4 has a crown flatness < 3 metres ➔ 50% of all trees
- Tree 2 grows < 1.3 metres/year ➔ 25% of all trees

Expected prevalence = $0.5\ x\ 0.5\ x\ 0.5\ x\ 0.25 = 0.03125 = 3.125\%$

Observed Prevalence

Here is a continuation on the theoretical example, with the focus on observed calculated.

How many percent of all trees fulfil all thresholds simultaneously:

- Higher than 10 metres
- Wider than 4 metres
- Flatter than 3 metres
- Grows less than 1.3 metres / year

From the expected prevalence, we know what trees fulfil what demand, but if we only look at the tree(s) that fulfils all thresholds:

- Tree 1 and 2 > 10 metres ➔ 50% of all trees
- Tree 2 and 3 has a crown width > 4 metres ➔ 50% of all trees
- Tree 2 and 4 has a crown flatness < 3 metres ➔ 50% of all trees
- Tree 2 grows < 1.3 metres/year ➔ 25% of all trees

It is evident that tree 2 is the only one that fulfils all thresholds, which means that:

Observed prevalence = tree 2 fulfils all thresholds simultaneously = 25%

LIFT – Ratio

Now that we know that:

Expected prevalence = 3.125% = 0.03125

Observed prevalence = 25% = 0.25

We can calculate LIFT as:

$$LIFT = \frac{Observed\ Prevalence}{Expected\ Prevalence}$$

$$LIFT = \frac{0.25}{0.03125} = 8$$

LIFT-Value

LIFT = 1 → The combination of traits occurs exactly as often as expected by chance
=> No structural signal is present

LIFT < 1 → The combination occurs less often than expected by chance
=> The thresholds are not meaningful and do not capture any realistic structure

LIFT > 1 → The combination occurs more often than expected by chance
=> A strong signal is present in the data, and the thresholds are relevant for identifying old trees

This is a simple way of exemplifying the process, but keep in mind that everything is theoretical. A forest of four trees is not probable, and the values presented is not rooted in real life either. However, it is a way of showing how LIFT works and how the method compares the observe prevalence and the expected prevalence.

Series from Lund University

Department of Physical Geography and Ecosystem Science

Master Thesis in Geographical Information Science

1. *Anthony Lawther:* The application of GIS-based binary logistic regression for slope failure susceptibility mapping in the Western Grampian Mountains, Scotland (2008).

2. *Rickard Hansen:* Daily mobility in Grenoble Metropolitan Region, France. Applied GIS methods in time geographical research (2008).

3. *Emil Bayramov:* Environmental monitoring of bio-restoration activities using GIS and Remote Sensing (2009).

4. *Rafael Villarreal Pacheco:* Applications of Geographic Information Systems as an analytical and visualization tool for mass real estate valuation: a case study of Fontibon District, Bogota, Columbia (2009).

5. *Siri Oestreich Waage:* a case study of route solving for oversized transport: The use of GIS functionalities in transport of transformers, as part of maintaining a reliable power infrastructure (2010).

6. *Edgar Pimiento:* Shallow landslide susceptibility – Modelling and validation (2010).

7. *Martina Schäfer:* Near real-time mapping of floodwater mosquito breeding sites using aerial photographs (2010).

8. *August Pieter van Waarden-Nagel:* Land use evaluation to assess the outcome of the programme of rehabilitation measures for the river Rhine in the Netherlands (2010).

9. *Samira Muhammad:* Development and implementation of air quality data mart for Ontario, Canada: A case study of air quality in Ontario using OLAP tool. (2010).

10. *Fredros Oketch Okumu*: Using remotely sensed data to explore spatial and temporal relationships between photosynthetic productivity of vegetation and malaria transmission intensities in selected parts of Africa (2011).

11. *Svajunas Plunge:* Advanced decision support methods for solving diffuse water pollution problems (2011).

12. *Jonathan Higgins:* Monitoring urban growth in greater Lagos: A case study using GIS to monitor the urban growth of Lagos 1990 - 2008 and produce future growth prospects for the city (2011).

13. *Mårten Karlberg:* Mobile Map Client API: Design and Implementation for Android (2011).

14. *Jeanette McBride:* Mapping Chicago area urban tree canopy using color infrared imagery (2011).

15. *Andrew Farina:* Exploring the relationship between land surface temperature and vegetation abundance for urban heat island mitigation in Seville, Spain (2011).

16. *David Kanyari*: Nairobi City Journey Planner: An online and a Mobile Application (2011).

17. *Laura V. Drews:* Multi-criteria GIS analysis for siting of small wind power plants - A case study from Berlin (2012).

18. *Qaisar Nadeem:* Best living neighborhood in the city - A GIS based multi criteria evaluation of ArRiyadh City (2012).

19. *Ahmed Mohamed El Saeid Mustafa:* Development of a photo voltaic building rooftop integration analysis tool for GIS for Dokki District, Cairo, Egypt (2012).

20. *Daniel Patrick Taylor*: Eastern Oyster Aquaculture: Estuarine Remediation via Site Suitability and Spatially Explicit Carrying Capacity Modeling in Virginia's Chesapeake Bay (2013).

21. *Angeleta Oveta Wilson:* A Participatory GIS approach to *unearthing* Manchester's Cultural Heritage '*gold mine'* (2013).

22. *Ola Svensson:* Visibility and Tholos Tombs in the Messenian Landscape: A Comparative Case Study of the Pylian Hinterlands and the Soulima Valley (2013).

23. *Monika Ogden:* Land use impact on water quality in two river systems in South Africa (2013).

24. *Stefan Rova:* A GIS based approach assessing phosphorus load impact on Lake Flaten in Salem, Sweden (2013).

25. *Yann Buhot:* Analysis of the history of landscape changes over a period of 200 years. How can we predict past landscape pattern scenario and the impact on habitat diversity? (2013).

26. *Christina Fotiou:* Evaluating habitat suitability and spectral heterogeneity models to predict weed species presence (2014).

27. *Inese Linuza:* Accuracy Assessment in Glacier Change Analysis (2014).

28. *Agnieszka Griffin:* Domestic energy consumption and social living standards: a GIS analysis within the Greater London Authority area (2014).

29. *Brynja Guðmundsdóttir:* Detection of potential arable land with remote sensing and GIS - A Case Study for Kjósarhreppur (2014).

30. *Oleksandr Nekrasov:* Processing of MODIS Vegetation Indices for analysis of agricultural droughts in the southern Ukraine between the years 2000-2012 (2014).

31. *Sarah Tressel:* Recommendations for a polar Earth science portal in the context of Arctic Spatial Data Infrastructure (2014).

32. *Caroline Gevaert:* Combining Hyperspectral UAV and Multispectral Formosat-2 Imagery for Precision Agriculture Applications (2014).

33. *Salem Jamal-Uddeen:* Using GeoTools to implement the multi-criteria evaluation analysis - weighted linear combination model (2014).

34. *Samanah Seyedi-Shandiz:* Schematic representation of geographical railway network at the Swedish Transport Administration (2014).

35. *Kazi Masel Ullah:* Urban Land-use planning using Geographical Information System and analytical hierarchy process: case study Dhaka City (2014).

36. *Alexia Chang-Wailing Spitteler:* Development of a web application based on MCDA and GIS for the decision support of river and floodplain rehabilitation projects (2014).

37. *Alessandro De Martino:* Geographic accessibility analysis and evaluation of potential changes to the public transportation system in the City of Milan (2014).

38. *Alireza Mollasalehi:* GIS Based Modelling for Fuel Reduction Using Controlled Burn in Australia. Case Study: Logan City, QLD (2015).

39. *Negin A. Sanati:* Chronic Kidney Disease Mortality in Costa Rica; Geographical Distribution, Spatial Analysis and Non-traditional Risk Factors (2015).

40. *Karen McIntyre:* Benthic mapping of the Bluefields Bay fish sanctuary, Jamaica (2015).

41. *Kees van Duijvendijk:* Feasibility of a low-cost weather sensor network for agricultural purposes: A preliminary assessment (2015).

42. *Sebastian Andersson Hylander:* Evaluation of cultural ecosystem services using GIS (2015).

43. *Deborah Bowyer:* Measuring Urban Growth, Urban Form and Accessibility as Indicators of Urban Sprawl in Hamilton, New Zealand (2015).

44. *Stefan Arvidsson:* Relationship between tree species composition and phenology extracted from satellite data in Swedish forests (2015).

45. *Damián Giménez Cruz*: GIS-based optimal localisation of beekeeping in rural Kenya (2016).

46. *Alejandra Narváez Vallejo:* Can the introduction of the topographic indices in LPJ-GUESS improve the spatial representation of environmental variables? (2016).

47. *Anna Lundgren:* Development of a method for mapping the highest coastline in Sweden using breaklines extracted from high resolution digital elevation models (2016).

48. *Oluwatomi Esther Adejoro:* Does location also matter? A spatial analysis of social achievements of young South Australians (2016).

49. *Hristo Dobrev Tomov:* Automated temporal NDVI analysis over the Middle East for the period 1982 - 2010 (2016).

50. *Vincent Muller:* Impact of Security Context on Mobile Clinic Activities A GIS Multi Criteria Evaluation based on an MSF Humanitarian Mission in Cameroon (2016).

51. *Gezahagn Negash Seboka:* Spatial Assessment of NDVI as an Indicator of Desertification in Ethiopia using Remote Sensing and GIS (2016).

52. *Holly Buhler:* Evaluation of Interfacility Medical Transport Journey Times in Southeastern British Columbia. (2016).

53. *Lars Ole Grottenberg*: Assessing the ability to share spatial data between emergency management organisations in the High North (2016).

54. *Sean Grant:* The Right Tree in the Right Place: Using GIS to Maximize the Net Benefits from Urban Forests (2016).

55. *Irshad Jamal:* Multi-Criteria GIS Analysis for School Site Selection in Gorno-Badakhshan Autonomous Oblast, Tajikistan (2016).

56. *Fulgencio Sanmartín:* Wisdom-volkano: A novel tool based on open GIS and time-series visualization to analyse and share volcanic data (2016).

57. *Nezha Acil:* Remote sensing-based monitoring of snow cover dynamics and its influence on vegetation growth in the Middle Atlas Mountains (2016).

58. *Julia Hjalmarsson:* A Weighty Issue: Estimation of Fire Size with Geographically Weighted Logistic Regression (2016).

59. *Mathewos Tamiru Amato:* Using multi-criteria evaluation and GIS for chronic food and nutrition insecurity indicators analysis in Ethiopia (2016).

60. *Karim Alaa El Din Mohamed Soliman El Attar:* Bicycling Suitability in Downtown, Cairo, Egypt (2016).

61. *Gilbert Akol Echelai:* Asset Management: Integrating GIS as a Decision Support Tool in Meter Management in National Water and Sewerage Corporation (2016).

62. *Terje Slinning:* Analytic comparison of multibeam echo soundings (2016).

63. *Gréta Hlín Sveinsdóttir:* GIS-based MCDA for decision support: A framework for wind farm siting in Iceland (2017).

64. *Jonas Sjögren:* Consequences of a flood in Kristianstad, Sweden: A GIS-based analysis of impacts on important societal functions (2017).

65. *Nadine Raska:* 3D geologic subsurface modelling within the Mackenzie Plain, Northwest Territories, Canada (2017).

66. *Panagiotis Symeonidis*: Study of spatial and temporal variation of atmospheric optical parameters and their relation with PM 2.5 concentration over Europe using GIS technologies (2017).

67. *Michaela Bobeck:* A GIS-based Multi-Criteria Decision Analysis of Wind Farm Site Suitability in New South Wales, Australia, from a Sustainable Development Perspective (2017).

68. *Raghdaa Eissa*: Developing a GIS Model for the Assessment of Outdoor Recreational Facilities in New Cities Case Study: Tenth of Ramadan City, Egypt (2017).

69. *Zahra Khais Shahid*: Biofuel plantations and isoprene emissions in Svea and Götaland (2017).

70. *Mirza Amir Liaquat Baig*: Using geographical information systems in epidemiology: Mapping and analyzing occurrence of diarrhea in urban - residential area of Islamabad, Pakistan (2017).

71. *Joakim Jörwall*: Quantitative model of Present and Future well-being in the EU-28: A spatial Multi-Criteria Evaluation of socioeconomic and climatic comfort factors (2017).

72. *Elin Haettner*: Energy Poverty in the Dublin Region: Modelling Geographies of Risk (2017).

73. *Harry Eriksson*: Geochemistry of stream plants and its statistical relations to soil- and bedrock geology, slope directions and till geochemistry. A GIS-analysis of small catchments in northern Sweden (2017).

74. *Daniel Gardevärn:* PPGIS and Public meetings – An evaluation of public participation methods for urban planning (2017).

75. *Kim Friberg:* Sensitivity Analysis and Calibration of Multi Energy Balance Land Surface Model Parameters (2017).

76. *Viktor Svanerud:* Taking the bus to the park? A study of accessibility to green areas in Gothenburg through different modes of transport (2017).

77. *Lisa-Gaye Greene*: Deadly Designs: The Impact of Road Design on Road Crash Patterns along Jamaica's North Coast Highway (2017).

78. *Katarina Jemec Parker*: Spatial and temporal analysis of fecal indicator bacteria concentrations in beach water in San Diego, California (2017).

79. *Angela Kabiru*: An Exploratory Study of Middle Stone Age and Later Stone Age Site Locations in Kenya's Central Rift Valley Using Landscape Analysis: A GIS Approach (2017).

80. *Kristean Björkmann*: Subjective Well-Being and Environment: A GIS-Based Analysis (2018).

81. *Williams Erhunmonmen Ojo*: Measuring spatial accessibility to healthcare for people living with HIV-AIDS in southern Nigeria (2018).

82. *Daniel Assefa*: Developing Data Extraction and Dynamic Data Visualization (Styling) Modules for Web GIS Risk Assessment System (WGRAS). (2018).

83. *Adela Nistora*: Inundation scenarios in a changing climate: assessing potential impacts of sea-level rise on the coast of South-East England (2018).

84. *Marc Seliger*: Thirsty landscapes - Investigating growing irrigation water consumption and potential conservation measures within Utah's largest master-planned community: Daybreak (2018).

85. *Luka Jovičić*: Spatial Data Harmonisation in Regional Context in Accordance with INSPIRE Implementing Rules (2018).

86. *Christina Kourdounouli*: Analysis of Urban Ecosystem Condition Indicators for the Large Urban Zones and City Cores in EU (2018).

87. *Jeremy Azzopardi*: Effect of distance measures and feature representations on distance-based accessibility measures (2018).

88. *Patrick Kabatha*: An open source web GIS tool for analysis and visualization of elephant GPS telemetry data, alongside environmental and anthropogenic variables (2018).

89. *Richard Alphonce Giliba*: Effects of Climate Change on Potential Geographical Distribution of Prunus africana (African cherry) in the Eastern Arc Mountain Forests of Tanzania (2018).

90. *Eiður Kristinn Eiðsson*: Transformation and linking of authoritative multi-scale geodata for the Semantic Web: A case study of Swedish national building data sets (2018).

91. *Niamh Harty*: HOP!: a PGIS and citizen science approach to monitoring the condition of upland paths (2018).

92. *José Estuardo Jara Alvear*: Solar photovoltaic potential to complement hydropower in Ecuador: A GIS-based framework of analysis (2018).

93. *Brendan O'Neill*: Multicriteria Site Suitability for Algal Biofuel Production Facilities (2018).

94. *Roman Spataru*: Spatial-temporal GIS analysis in public health – a case study of polio disease (2018).

95. *Alicja Miodońska*: Assessing evolution of ice caps in Suðurland, Iceland, in years 1986 - 2014, using multispectral satellite imagery (2019).

96. *Dennis Lindell Schettini*: A Spatial Analysis of Homicide Crime's Distribution and Association with Deprivation in Stockholm Between 2010-2017 (2019).

97. *Damiano Vesentini*: The Po Delta Biosphere Reserve: Management challenges and priorities deriving from anthropogenic pressure and sea level rise (2019).

98. *Emilie Arnesten*: Impacts of future sea level rise and high water on roads, railways and environmental objects: a GIS analysis of the potential effects of increasing sea levels and highest projected high water in Scania, Sweden (2019).

99. *Syed Muhammad Amir Raza*: Comparison of geospatial support in RDF stores: Evaluation for ICOS Carbon Portal metadata (2019).

100. *Hemin Tofiq*: Investigating the accuracy of Digital Elevation Models from UAV images in areas with low contrast: A sandy beach as a case study (2019).

101. *Evangelos Vafeiadis*: Exploring the distribution of accessibility by public transport using spatial analysis. A case study for retail concentrations and public hospitals in Athens (2019).

102. *Milan Sekulic*: Multi-Criteria GIS modelling for optimal alignment of roadway by-passes in the Tlokweng Planning Area, Botswana (2019).

103. *Ingrid Piirisaar*: A multi-criteria GIS analysis for siting of utility-scale photovoltaic solar plants in county Kilkenny, Ireland (2019).

104. *Nigel Fox*: Plant phenology and climate change: possible effect on the onset of various wild plant species' first flowering day in the UK (2019).

105. *Gunnar Hesch*: Linking conflict events and cropland development in Afghanistan, 2001 to 2011, using MODIS land cover data and Uppsala Conflict Data Programme (2019).

106. *Elijah Njoku*: Analysis of spatial-temporal pattern of Land Surface Temperature (LST) due to NDVI and elevation in Ilorin, Nigeria (2019).

107. *Katalin Bunyevácz*: Development of a GIS methodology to evaluate informal urban green areas for inclusion in a community governance program (2019).

108. *Paul dos Santos*: Automating synthetic trip data generation for an agent-based simulation of urban mobility (2019).

109. *Robert O' Dwyer*: Land cover changes in Southern Sweden from the mid-Holocene to present day: Insights for ecosystem service assessments (2019).

110. *Daniel Klingmyr*: Global scale patterns and trends in tropospheric NO2 concentrations (2019).

111. *Marwa Farouk Elkabbany*: Sea Level Rise Vulnerability Assessment for Abu Dhabi, United Arab Emirates (2019).

112. *Jip Jan van Zoonen*: Aspects of Error Quantification and Evaluation in Digital Elevation Models for Glacier Surfaces (2020).

113. *Georgios Efthymiou*: The use of bicycles in a mid-sized city – benefits and obstacles identified using a questionnaire and GIS (2020).

114. *Haruna Olayiwola Jimoh*: Assessment of Urban Sprawl in MOWE/IBAFO Axis of Ogun State using GIS Capabilities (2020).

115. *Nikolaos Barmpas Zachariadis*: Development of an iOS, Augmented Reality for disaster management (2020).

116. *Ida Storm*: ICOS Atmospheric Stations: Spatial Characterization of CO2 Footprint Areas and Evaluating the Uncertainties of Modelled CO2 Concentrations (2020).

117. *Alon Zuta*: Evaluation of water stress mapping methods in vineyards using airborne thermal imaging (2020).

118. *Marcus Eriksson*: Evaluating structural landscape development in the municipality Upplands-Bro, using landscape metrics indices (2020).

119. *Ane Rahbek Vierø*: Connectivity for Cyclists? A Network Analysis of Copenhagen's Bike Lanes (2020).

120. *Cecilia Baggini*: Changes in habitat suitability for three declining Anatidae species in saltmarshes on the Mersey estuary, North-West England (2020).

121. *Bakrad Balabanian*: Transportation and Its Effect on Student Performance (2020).

122. *Ali Al Farid*: Knowledge and Data Driven Approaches for Hydrocarbon Microseepage Characterizations: An Application of Satellite Remote Sensing (2020).

123. *Bartlomiej Kolodziejczyk*: Distribution Modelling of Gene Drive-Modified Mosquitoes and Their Effects on Wild Populations (2020).

124. *Alexis Cazorla*: Decreasing organic nitrogen concentrations in European water bodies - links to organic carbon trends and land cover (2020).

125. *Kharid Mwakoba*: Remote sensing analysis of land cover/use conditions of community-based wildlife conservation areas in Tanzania (2021).

126. *Chinatsu Endo*: Remote Sensing Based Pre-Season Yellow Rust Early Warning in Oromia, Ethiopia (2021).

127. *Berit Mohr*: Using remote sensing and land abandonment as a proxy for long-term human out-migration. A Case Study: Al-Hassakeh Governorate, Syria (2021).

128. *Kanchana Nirmali Bandaranayake*: Considering future precipitation in delineation locations for water storage systems - Case study Sri Lanka (2021).

129. *Emma Bylund*: Dynamics of net primary production and food availability in the aftermath of the 2004 and 2007 desert locust outbreaks in Niger and Yemen (2021).

130. *Shawn Pace*: Urban infrastructure inundation risk from permanent sea-level rise scenarios in London (UK), Bangkok (Thailand) and Mumbai (India): A comparative analysis (2021).

131. *Oskar Evert Johansson*: The hydrodynamic impacts of Estuarine Oyster reefs, and the application of drone technology to this study (2021).

132. *Pritam Kumarsingh*: A Case Study to develop and test GIS/SDSS methods to assess the production capacity of a Cocoa Site in Trinidad and Tobago (2021).

133. *Muhammad Imran Khan*: Property Tax Mapping and Assessment using GIS (2021).

134. *Domna Kanari*: Mining geosocial data from Flickr to explore tourism patterns: The case study of Athens (2021).

135. *Mona Tykesson Klubien*: Livestock-MRSA in Danish pig farms (2021).

136. *Ove Njøten*: Comparing radar satellites. Use of Sentinel-1 leads to an increase in oil spill alerts in Norwegian waters (2021).

137. *Panagiotis Patrinos*: Change of heating fuel consumption patterns produced by the economic crisis in Greece (2021).

138. *Lukasz Langowski*: Assessing the suitability of using Sentinel-1A SAR multi-temporal imagery to detect fallow periods between rice crops (2021).

139. *Jonas Tillman*: Perception accuracy and user acceptance of legend designs for opacity data mapping in GIS (2022).

140. *Gabriela Olekszyk*: ALS (Airborne LIDAR) accuracy: Can potential low data quality of ground points be modelled/detected? Case study of 2016 LIDAR capture over Auckland, New Zealand (2022).

141. *Luke Aspland*: Weights of Evidence Predictive Modelling in Archaeology (2022).

142. *Luís Fareleira Gomes*: The influence of climate, population density, tree species and land cover on fire pattern in mainland Portugal (2022).

143. *Andreas Eriksson*: Mapping Fire Salamander (Salamandra salamandra) Habitat Suitability in Baden-Württemberg with Multi-Temporal Sentinel-1 and Sentinel-2 Imagery (2022).

144. *Lisbet Hougaard Baklid*: Geographical expansion rate of a brown bear population in Fennoscandia and the factors explaining the directional variations (2022).

145. *Victoria Persson*: Mussels in deep water with climate change: Spatial distribution of mussel (Mytilus galloprovincialis) growth offshore in the French Mediterranean with respect to climate change scenario RCP 8.5 Long Term and Integrated Multi-Trophic Aquaculture (IMTA) using Dynamic Energy Budget (DEB) modelling (2022).

146. *Benjamin Bernard Fabien Gérard Borgeais*: Implementing a multi-criteria GIS analysis and predictive modelling to locate Upper Palaeolithic decorated caves in the Périgord noir, France (2022).

147. *Bernat Dorado-Guerrero*: Assessing the impact of post-fire restoration interventions using spectral vegetation indices: A case study in El Bruc, Spain (2022).

148. *Ignatius Gabriel Aloysius Maria Perera*: The Influence of Natural Radon Occurrence on the Severity of the COVID-19 Pandemic in Germany: A Spatial Analysis (2022).

149. *Mark Overton*: An Analysis of Spatially-enabled Mobile Decision Support Systems in a Collaborative Decision-Making Environment (2022).

150. *Viggo Lunde*: Analysing methods for visualizing time-series datasets in open-source web mapping (2022).

151. *Johan Viscarra Hansson*: Distribution Analysis of Impatiens glandulifera in Kronoberg County and a Pest Risk Map for Alvesta Municipality (2022).

152. *Vincenzo Poppiti*: GIS and Tourism: Developing strategies for new touristic flows after the Covid-19 pandemic (2022).

153. *Henrik Hagelin*: Wildfire growth modelling in Sweden - A suitability assessment of available data (2023).

154. *Gabriel Romeo Ferriols Pavico*: Where there is road, there is fire (influence): An exploratory study on the influence of roads in the spatial patterns of Swedish wildfires of 2018 (2023).

155. *Colin Robert Potter*: Using a GIS to enable an economic, land use and energy output comparison between small wind powered turbines and large-scale wind farms: the case of Oslo, Norway (2023).

156. *Krystyna Muszel*: Impact of Sea Surface Temperature and Salinity on Phytoplankton blooms phenology in the North Sea (2023).

157. *Tobias Rydlinge*: Urban tree canopy mapping - an open source deep learning approach (2023).

158. *Albert Wellendorf*: Multi-scale Bark Beetle Predictions Using Machine Learning (2023).

159. *Manolis Papadakis*: Use of Satellite Remote Sensing for Detecting Archaeological Features: An Example from Ancient Corinth, Greece (2023).

160. *Konstantinos Sourlamtas*: Developing a Geographical Information System for a water and sewer network, for monitoring, identification and leak repair - Case study: Municipal Water Company of Naoussa, Greece (2023).

161. *Xiaoming Wang*: Identification of restoration hotspots in landscape-scale green infrastructure planning based on model-predicted connectivity forest (2023).

162. *Sarah Sienaert*: Usability of Sentinel-1 C-band VV and VH SAR data for the detection of flooded oil palm (2023).

163. *Katarina Ekeroot*: Uncovering the spatial relationships between Covid-19 vaccine coverage and local politics in Sweden (2023).

164. *Nikolaos Kouskoulis*: Exploring patterns in risk factors for bark beetle attack during outbreaks triggered by drought stress with harvester data on attacked trees: A case study in Southeastern Sweden (2023).

165. *Jonas Almén*: Geographic polarization and clustering of partisan voting: A local-level analysis of Stockholm Municipality (2023).

166. *Sara Sharon Jones*: Tree species impact on Forest Fire Spread Susceptibility in Sweden (2023).

167. *Takura Matswetu*: Towards a Geographic Information Systems and Data-Driven Integration Management. Studying holistic integration through spatial accessibility of services in Tampere, Finland. (2023).

168. *Duncan Jones*: Investigating the influence of the tidal regime on harbour porpoise *Phocoena phocoena* distribution in Mount's Bay, Cornwall (2023).

169. *Jason Craig Joubert*: A comparison of remote sensed semi-arid grassland vegetation anomalies detected using MODIS and Sentinel-3, with anomalies in ground-based eddy covariance flux measurements (2023).

170. *Anastasia Sarelli*: Land cover classification using machine-learning techniques applied to fused multi-modal satellite imagery and time series data (2024).

171. *Athanasios Senteles*: Integrating Local Knowledge into the Spatial Analysis of Wind Power: The case study of Northern Tzoumerka, Greece (2024).

172. *Rebecca Borg:* Using GIS and satellite data to assess access of green area for children living in growing cities (2024).

173. *Panagiotis–Dimitrios Tsachageas*: Multicriteria Evaluation in Real Estate Land-use Suitability Analysis: The case of Volos, Greece (2024).

174. *Hugo Nilsson*: Inferring lane-level topology of signalised intersections from aerial imagery and OpenStreetMap using deep learning (2024).

175. *Pavlos Alexantonakis*: Estimating lake water volume fluctuations using Sentinel-2 and ICESat-2 remote sensing data (2024).

176. *Karl-Martin Wigen*: Physical barriers and where to find them (2024).

177. *Martin Storsnes*: Temporal RX-algorithm performance on Sentinel-2 images (2024).

178. *Saulė Gabrielė Petraitytė*: The Relation Between Covid-19 Vaccination and Voting Trends in Lithuania: A Spatial Analysis (2024).

179. *Pedro Martinez Duran*: Olive yield forecasting from remote sensing and climate datasets in the Jaen province (Spain) (2024).

180. *Josefine Kynde Hämberg*: Proximity to Urban Green Spaces for Older Adults in Specific Housings - a Case Study of Malmö, Sweden (2024).

181. *Max Bengtsson*: A Site Selection of An Energy Island in the North Sea: Optimal Location in an Ecological and an Economic Scenario Using a Multicriteria Decision Analysis (MCDA) (2024).

182. *Anna Börmann*: Assessing Great Britain as a relocation site for the threatened Iberian Lynx in a changing climate (2024).

183. *Josephine Roosli*: Flood Risk Assessment for the Kävlinge River for Present and Future Climate Scenarios using HEC-RAS Rain-on-Grid (2024).

184. *Seán Flanagan*: Spatiotemporal dynamics of E-scooter sharing ridership and their associations with the built environment: A Swedish comparative study (2024).

185. *Wouter Vorsters*: Assessing the Impact of Combined Sewer Overflow on the Habitat of Lampetra planeri: A Case Study in Flanders, Belgium (2025).

186. *Kathleen Macdonald*: Cetacean strandings on the Scottish coast: coastal accessibility factors lead to underreporting (2025).

187. *Athanasios Emmanouil Mourampetzis*: Navigating the Shadows: A Comparative Analysis of SAR and Optical Imagery for Detecting (Dark) Vessels (2025).

188. *Nizam-ud-Din*: Spatial Land Records System using Geospatial Techniques: a case study of a Mid-Sized Village in Pakistan (2025).

189. *Nedim Nasic Kjellgren*: Linked Geodata: Improving Rooftop Photovoltaic Production Estimates through BIM-GIS Integration using Semantic Web Technologies (2025).

190. *Vedrana Pretkovic*: Spatio-temporal vegetation changes in the Pacific-Chocó region of Colombia during the conflict and post-conflict periods (2025).

191. *Evelina Bengtsson*: A Socioeconomic Dimension of Crime: A Spatial Study of Firearm-related Violence in Malmö (2025).

192. *Martynas Bielinis*: Application of C-band Radar Interferometry for Dune Monitoring in the Curonian Spit (2025).

193. *Paulina Magdalena Rieke*: Case study of the benefits of BIM and GIS solutions used on a live infrastructure project (2025).

194. *Alina Schärer*: Evaluating the Impact of Urban Green Spaces and Vegetation Characteristics on Land Surface Temperature Across Swiss Cities Using Machine Learning (2025).

195. *Paul Stewart:* Where is wild in Glasgow's Southside? A test of the applicability of relative wildness mapping to suburban Scotland (2025).

196. *Georgios Fylakis:* Spatiotemporal analysis of the integration between shared e-scooters and public transport: Case studies in Oslo and Stockholm (2025).

197. *Andreas Klasson*: Generating 3D building models according to Swedish building specification using footprints and airborne laser scanning (2025).

198. *Agaton Järemo Lawin*: The spread of Japanese knotweed in Scania: Invasion suitability prediction using species distribution modelling (2025).

199. *Jesse Stewart:* Contextualizing the Geographic Influence on Infantry Manoeuvrability in a Historical Battlefield Using GIS: A Case Study of the Canadian Corps in the Second Battle of Passchendaele, First World War (2025).

200. *Oskar Vejkdal Thorsberg*: Automatic geometry extraction in digital building permits: A case study using BIM and NS Building (2025).

201. *Spyridon Gerafentis*: Impact of the COVID-19 "Lockdown" on Air Quality in Athens (2025).

202. *Symeon Andriotis*: Political Violence in Athens, Greece (2008-2024): A Machine Learning Approach for Predictive Modelling of Spatial Risk Patterns (2025).

203. *Simon Westman*: Detecting Structurally Old Scots Pine: A Crown-Metric Approach Using National ALS and LIFT Enrichment (2026).